

ESD RECORD COPY

RETURN TO
SCIENTIFIC & TECHNICAL INFORMATION DIVISION
(ESTI), BUILDING 1211

ESD ACCESSION LIST

ESTI Call No. AL 59102

Copy No. / of / cys.

EDS-TR-67-597
FILE COPY

Semiannual Technical Summary

Seismic Discrimination

31 December 1967

Prepared for the Advanced Research Projects Agency
under Electronic Systems Division Contract AF 19(628)-5167 by

Lincoln Laboratory

MASSACHUSETTS INSTITUTE OF TECHNOLOGY

Lexington, Massachusetts



A100664872

The work reported in this document was performed at Lincoln Laboratory, a center for research operated by Massachusetts Institute of Technology. This research is a part of Project Vela Uniform, which is sponsored by the U.S. Advanced Research Projects Agency of the Department of Defense; it is supported by ARPA under Air Force Contract AF 19(628)-5167 (ARPA Order 512).

This report may be reproduced to satisfy needs of U.S. Government agencies.

This document has been approved for public release and sale; its distribution is unlimited.

Non-Lincoln Recipients

PLEASE DO NOT RETURN

Permission is given to destroy this document
when it is no longer needed.

MASSACHUSETTS INSTITUTE OF TECHNOLOGY
LINCOLN LABORATORY

SEISMIC DISCRIMINATION

SEMIANNUAL TECHNICAL SUMMARY REPORT
TO THE
ADVANCED RESEARCH PROJECTS AGENCY

1 JULY - 31 DECEMBER 1967

ISSUED 30 JANUARY 1968

LEXINGTON

MASSACHUSETTS

ABSTRACT

Seismic source identification studies have continued during the present reporting period, using a single large array (the Montana LASA), while initial construction, design, and seismic surveying have proceeded for a possible second large array in Norway to work jointly with the LASA and other stations. Work on improving the convenience of machine seismic signal processing is reported, as well as research on earth structure, microseismic noise, and the measurement of long-baseline earth strain using laser interferometers.

Accepted for the Air Force
Franklin C. Hudson
Chief, Lincoln Laboratory Office

SUMMARY

This is the eighth Semiannual Technical Summary on Lincoln Laboratory's work for the Advanced Research Projects Agency on the seismic discrimination problem (Vela Uniform).

During this reporting period, work was more or less completed on identification techniques using data from the long-period (LP) portion of the Montana LASA as it now stands (Sec. I-B). Emphasis is shifting toward improving short-period (SP) capability (Sec. I-A) so that the virtually complete separation of blasts and earthquakes afforded by LP data (above magnitude $m_b = 4\frac{1}{2}$ to 5) can be extended to lower magnitudes at which surface waves are undetected, but above the SP detection threshold ($3\frac{1}{2}$). Results are reported (Sec. II) on the ability to locate epicenters from a single LASA by beamsplitting, an important part of the identification procedure, particularly for small magnitude events invisible at other stations.

The first SP subarray of a projected large array in Norway has been partly completed, preliminary signal and noise analyses made, and a design study made of the long-period portion of the array (Sec. IV).

The application to a variety of geophysical problems of digital recording and automatic and semiautomatic computer processing is under continued investigation and refinement (Sec. V). During this reporting period, progress has been made in greatly improving the convenience of signal handling operations through the use of a seismic data analysis console, a small general-purpose machine with appropriate hardware and software for real-time man-machine-data interaction.

Seismological research work in the program (Sec. VI) involves a continuation of effort on problems of earth structure and the nature of the microseismic noise, as well as a new one, the measurement of earth strains over several-kilometer atmospheric paths using laser interferometers.

A cumulative list of our publications forms Sec. VII.

P. E. Green

CONTENTS

Abstract	iii
Summary	iv
Glossary	vi
I. IDENTIFICATION	1
A. Study of Short-Period Discriminants	1
B. Long-Period Discriminants	3
II. LASA DETECTION AND LOCATION	8
III. MONTANA ARRAY	9
IV. NORWAY ARRAY	11
A. Norway Seismic Survey Installation	11
B. Noise and Signal Site Survey Results	11
C. Long-Period Array Design	15
V. GEOPHYSICAL DATA HANDLING TECHNIQUES	17
A. Data Analysis Console	17
B. Tsunami Warning Using a Single Large Array	20
VI. SEISMOLOGICAL RESEARCH	23
A. Crustal Structure Under Montana Lasa Inferred From Station Anomalies	23
B. Montana Noise Structure	27
C. Laser Interferometer Earth Strain Measurement	30
VII. CUMULATIVE LIST OF PUBLICATIONS	41

GLOSSARY

AFOSR	Air Force Office of Scientific Research
AFTAC	Air Force Technical Applications Center
ARPA	Advanced Research Projects Agency
BED	Beamformer-Event Detector
CRO	Cathode-Ray Oscilloscope
ERI	Earthquake Research Institute (University of Tokyo)
FASTABUL	Fast Automatic STATION BULLETIN
GMT	Greenwich Mean Time
LASA	Large Aperture Seismic Array
LDC	LASA Data Center
SATSR	Semiannual Technical Summary Report
SEM	Subarray Electronics Module
SNR	Signal-to-Noise Ratio
USCGS	United States Coast and Geodetic Survey

SEISMIC DISCRIMINATION

I. IDENTIFICATION

A. STUDY OF SHORT-PERIOD DISCRIMINANTS

It was mentioned in the June 1967 Semiannual Technical Summary on Seismic Discrimination (Sec. II-B) that LASA data were being collected on a reference population of events from the Sino-Soviet bloc area in order to provide a basis for the evaluation of various discriminants. Recordings of events, sent from the LASA Data Center in Billings, Montana, for possible inclusion in this population, were subjected to the following sequence of operations. First, a pattern of beams was formed (from subarray sums) surrounding the tentative epicenter reported on the LASA station bulletin. From playouts of these beams, a best one was chosen and its coordinates used as a revised epicenter. In some cases this process was iterated, using a beam pattern with a finer grid spacing. The final epicenter was then used to form a beam by steering the entire array of 525 elements. In some cases this beam was reformed by using time-delays which were manually determined by aligning traces (to compensate for inadequate station corrections). This final beam waveform was plotted, with and without bandpass filtering, and used for the manual measurement of amplitude and dominant period of P and (if present) pP. If pP was detected, its delay after P was also recorded. Complexity and spectral ratio were automatically measured on the beam outputs and magnitude determined from the P-measurements.

One hundred earthquakes and 19 explosions have been fully processed so far, and a report (under the title of this section) is in preparation describing the behavior of several discriminants on this population. The chief results can be summarized as follows:

- (1) A plot of cumulative number of detections vs magnitude yields a 75-percent cumulative detection probability at magnitude 4.45 for this population.
- (2) Although all the events were relocated by the beamforming process described above (and by checking the USCGS epicenters which were available for 60 of the 119 events), only a few were finally removed from the population because their epicenters were outside the area of interest. In other words, preliminary screening on the basis of the bulletin epicenter seems to be satisfactory.
- (3) Even though some screening out of deep events was performed at the LASA Data Center, 49 percent of the processed earthquakes proved to have measureable pP phases on the final beam.
- (4) The remaining population of presumably shallow events is not entirely satisfactory for discriminant evaluation, since it contains mostly large explosions and small earthquakes with relatively little overlap in magnitude range. However, spectral ratio appears to be quite promising, since a perfect separation of earthquakes and explosions was attained by plotting spectral ratio vs magnitude (Fig. 1). In an analogous plot of complexity vs magnitude, only about half the earthquakes are rejected (Fig. 2).

Section I

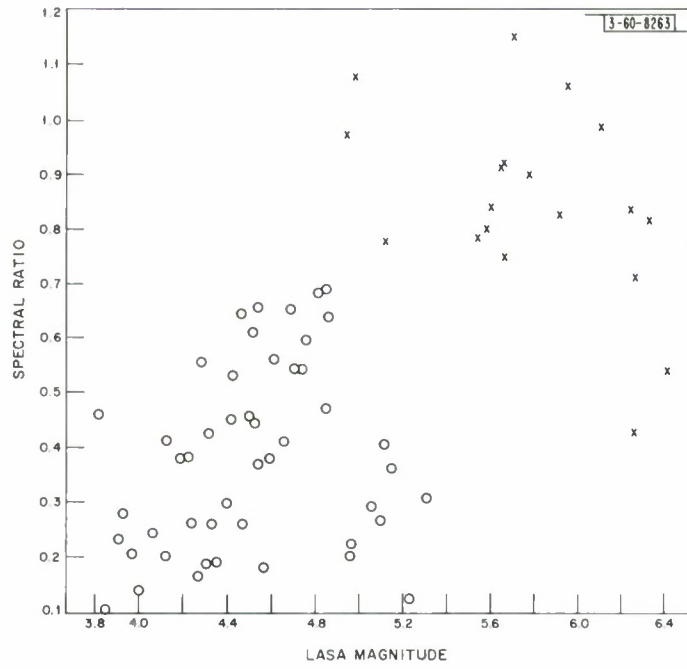


Fig. 1. Short-period spectral ratio vs magnitude for shallow earthquakes (o) and presumed explosions (x).

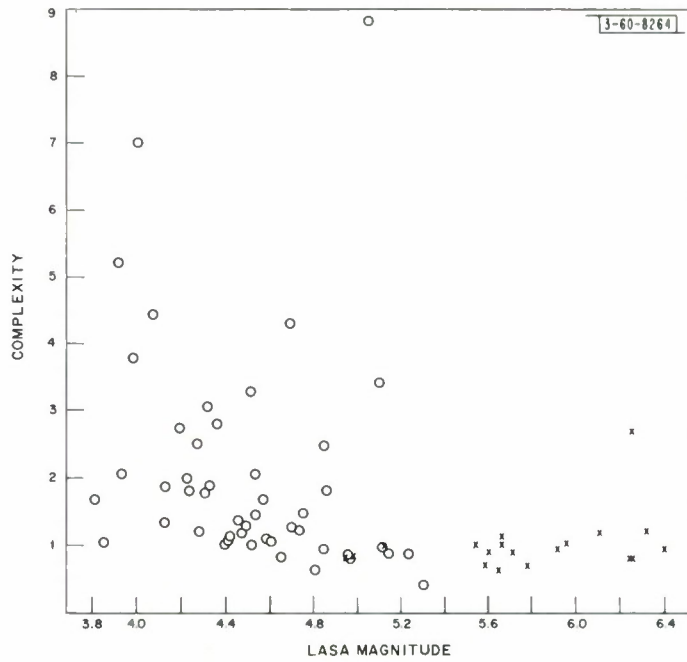


Fig. 2. Complexity vs magnitude for shallow earthquakes (o) and presumed explosions (x).

- (5) By separating our population into events occurring in the Kurile-Kamohatka region and all others (entirely continental), it was observed that the distribution of values of the spectral ratio was significantly different for the two groups. The complexity varied only slightly between the two. The implication is that discrimination criteria should be dependent on source region. When our population of earthquakes is restricted to continental, presumably shallow events, the source separation achieved by spectral ratio is improved.

It is planned to enlarge this reference population and continue the study of discriminants. In particular, certain techniques for the separation of populations using several discriminants simultaneously will be tried, as soon as a population is obtained which does not separate perfectly on spectral ratio alone. Long-period measurements will also be made and combined with the SP discriminants (LP data were available on only a fraction of the population described above, and perfect source separation was attained by plotting body-wave vs surface-wave magnitude, when the latter was available).

E. J. Kelly
R. T. Laeoss
R. M. Sheppard

B. LONG-PERIOD DISCRIMINANTS

The experiment to determine the effectiveness of a single LASA in using the surface-wave vs body-wave magnitude discriminant at teleseismic distances has been completed and the results published as part of a report summarizing a number of experiments with Montana LP data.¹ The following is a brief summary of the identification results.

The body-wave magnitude (m_b) and surface-wave magnitude (M_s) for events from four tectonic regions of the earth were computed using the method described in the last semiannual technical summary. The weaker events were subjected to both maximum-likelihood and delay-and-sum processing, which achieved about 14 and 11 db of SNR enhancement, respectively. In addition, if required, matched filtering was used to achieve another 6 to 10 db of SNR enhancement.

If matched filtering is required to detect the Rayleigh surface waves, then its output must be used to compute the surface-wave magnitude. This is done by calibrating the output of the matched filter for events which are visible, before the matched filtering is performed, from the desired epicentral region. A surface wave is said to be detected at the output of the matched filter if, at the computed arrival time, it exceeds a threshold level which is 6 db above the RMS noise level. It can be shown that this procedure leads to a 10-percent probability that noise alone has exceeded the threshold.

The results of the experiment are given in Figs. 3(a-e) which show M_s vs m_b for various regions, as well as the Gutenberg-Richter empirical relationship $M_s = 1.59 m_b - 3.97$. The results of Fig. 3 are very encouraging since there is a perfect and wide separation between the earthquake and explosion populations for the Central Asian events [Fig. 3(a)]. The results obtained for the other epicentral regions in Figs. 3(b) - (d) show that these regions give rise to earthquakes for which the M_s vs m_b characteristic is somewhat different from that of the Central Asian area. In fact, the separation between these earthquakes and the Central Asian explosions

Section I

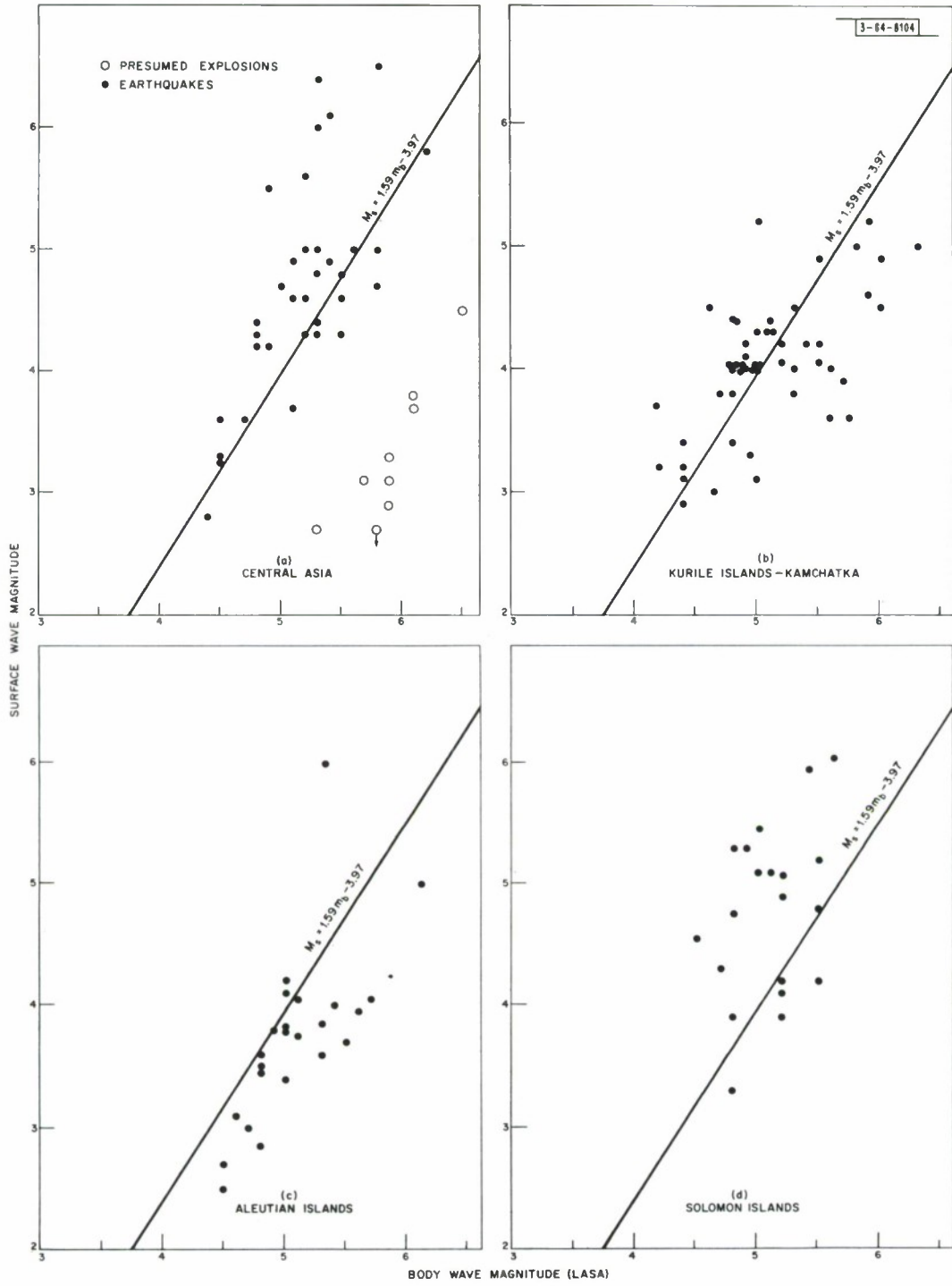


Fig. 3. Surface-wave vs body-wave magnitudes for earthquakes in four regions and presumed explosions in one region.

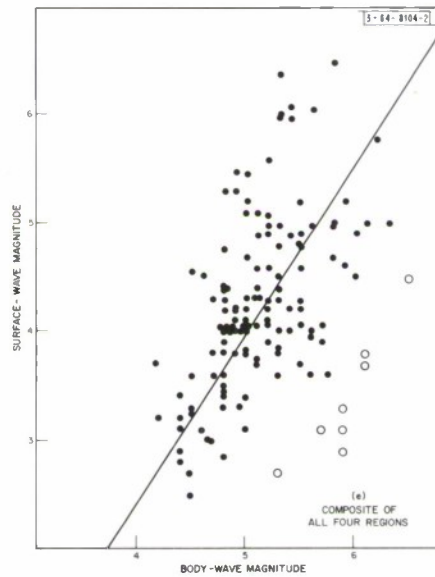


Fig. 3. Continued.

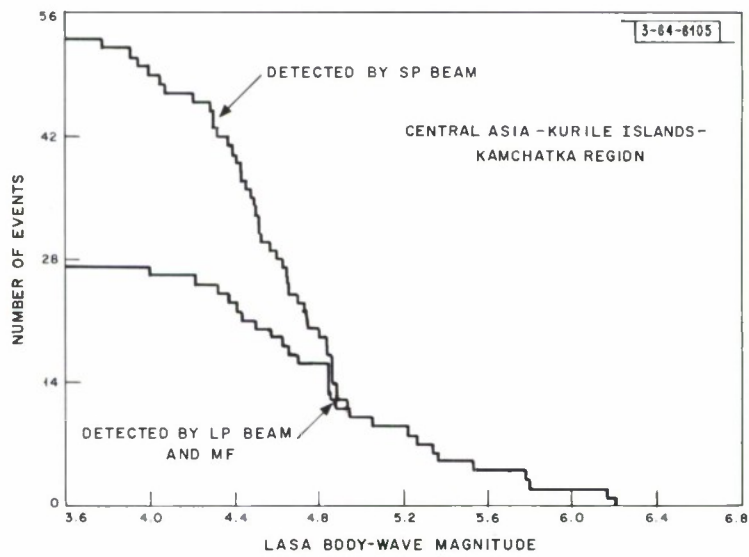


Fig. 4. Cumulative histograms comparing number of events detected on SP beam and LP beam plus matched filter.

Section I

appears to be worse for these other regions than that found for the Central Asian region. This has also been noted in a recent study of Aleutian earthquakes and the Aleutian underground nuclear explosion, Longshot,² and several other recent works.^{3,4}

The body-wave magnitude shown in Figs. 3(a-e) was determined by averaging over several widely separated sensors at LASA, so that a relatively good determination of body-wave magnitude is obtained, compared with that which would be obtained at a single conventional station. It should be mentioned that the surface-wave magnitude data given in Figs. 3(a-c) were also plotted vs the USCGS body-wave magnitude, and gave a similar separation between explosions and earthquakes.

An estimate was made of the detection threshold at LASA for LP Rayleigh surface waves for natural seismic events from the Central Asia-Kurile Islands-Kamchatka region. A selection of events from this region for which pP was not observed on LASA data from December 1966 to the end of April 1967 was used as a reference population of events. Approximately 53 events were included ranging in body-wave magnitude from 3.7 to 6.5. The P-wave for the events was detected by using an SP beam and the Rayleigh surface waves were detected by using an LP beam and matched filtering. The results of the experiment are given in Fig. 4, which shows the cumulative distribution of the events detected. It is seen that at $m_b = 4.5$, and 4.9 at LASA, 60 and 100-percent detectability of Rayleigh surface waves is achieved, respectively.

Several LP discriminants other than M_s vs m_b were investigated but proved less interesting because when they work at all, they do so at magnitudes so high that a simple M_s vs m_b determination should suffice. The criteria investigated were Love-wave excitation and use of Rayleigh waves for depth determination.

The threshold of observability in Montana of Love waves proved to be considerably higher than that for Rayleigh waves, partly because of the higher noise levels in the Montana LP horizontal sensors (see Sec. VI-B).

We investigated the use of M_s vs m_b or the dominant period of the Rayleigh phase for depth determination as part of a study of tsunami warning techniques⁵ (Sec. V-B). The results are shown in Figs. 5 and 6, respectively. The disparity between M_s and m_b should be depth dependent since, for an earthquake of given energy, the apparent m_b (i.e., m_b uncorrected for depth) should increase and the apparent surface-wave magnitude decrease as focal depth increases. Figure 5, giving apparent M_s and m_b readings for a number of Pacific and circum-Pacific earthquakes, shows a large scatter, and a depth dependence which, although present, is quite weak. For example, the data suggest that using an arbitrary decision rule that any event lying above the dashed line is shallower than 100 km and anything below is deeper, 67 percent of those having $h < 100$ and 67 percent of those having $h > 100$ would have been correctly labeled.

The second approach is based on the assumption that there is a general shift of the spectral concentration of surface-wave energy toward longer periods for increasing depth.⁶ Figure 6 shows data in the form of P_M , the period of maximum LASA surface-wave amplitude, vs focal depth reported by USCGS. A general increase of P_M with depth is seen, although the scatter is quite severe.

J. Capon
R. J. Greenfield

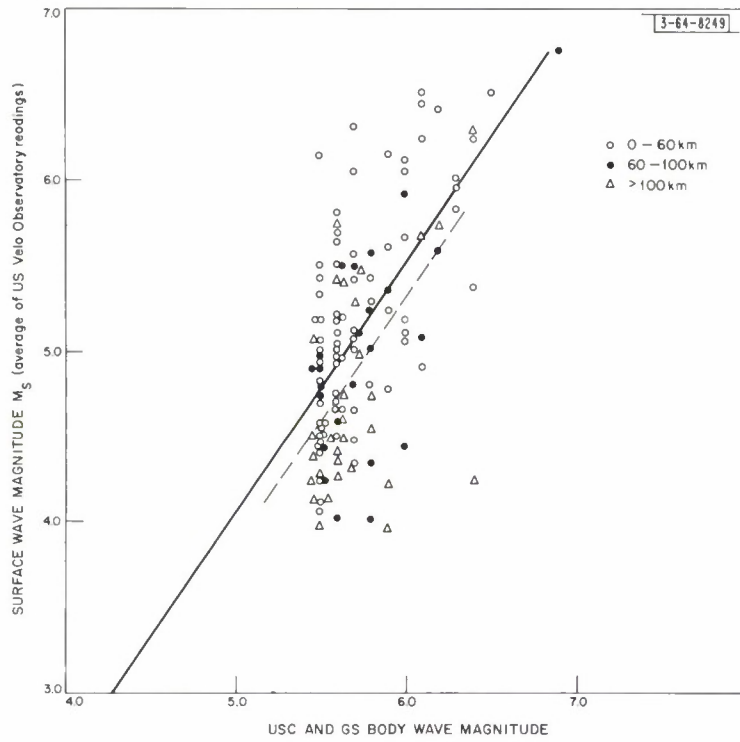


Fig. 5. Surface-wave magnitude M_s vs body-wave magnitude m_b for Pacific and circum-Pacific events in three depth ranges. (Velo array readings. An event-by-event comparison with LASA observations on 20 earthquakes showed no significant differences.)

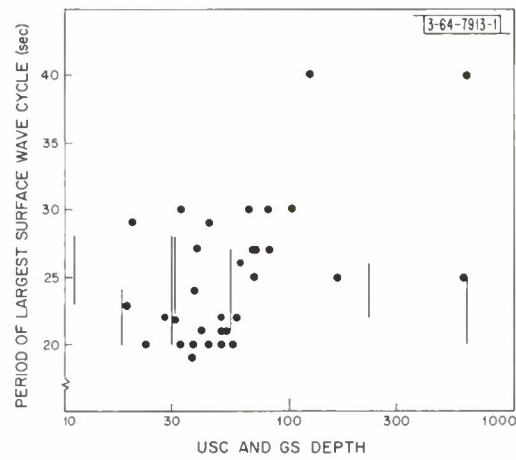


Fig. 6. Dependence of dominant surface-wave period P_M on depth.

II. LASA DETECTION AND LOCATION

The aperture of LASA provides the ability to form beams with a fairly small main lobe, and to determine epicenters by "beamsplitting."⁷ This is done as follows. The outputs of the sub-array straight sums are added after proper steering delays and station corrections have been applied, thus steering one beam toward a particular point on the earth's surface. When several hundred beams are formed and steered at spaced points surrounding a small epicentral region, the output power of the teleseismic P-wave signal can be measured and then contoured. The process can be repeated using a small beam spacing centered around the best beam from the previous run. The location of the beam that produces the highest signal power is then considered to be the epicenter of the event. This process should yield fairly accurate epicenters even for smaller magnitude events.

By using a small population of events from Honshu, Japan, epicenters were computed from local observations at the Earthquake Research Institute tripartite on Honshu and by beamsplitting of Montana data. A grid of beams was formed to cover the epicenter indicated by the local data or by the USCGS when it was available. The beams were separated by 0.5 degree and covered the area immediately around the supposed epicenter. The beam with the highest signal power was then considered to be the correct epicenter. In every case the beamsplit epicenter was slightly different from the original epicenter. A plot of the epicentral differences is shown in Fig. 7. The dashed curve indicates what the theoretical error in epicenters should be, assuming a particular model of the noise and perfect station corrections.

R. M. Sheppard

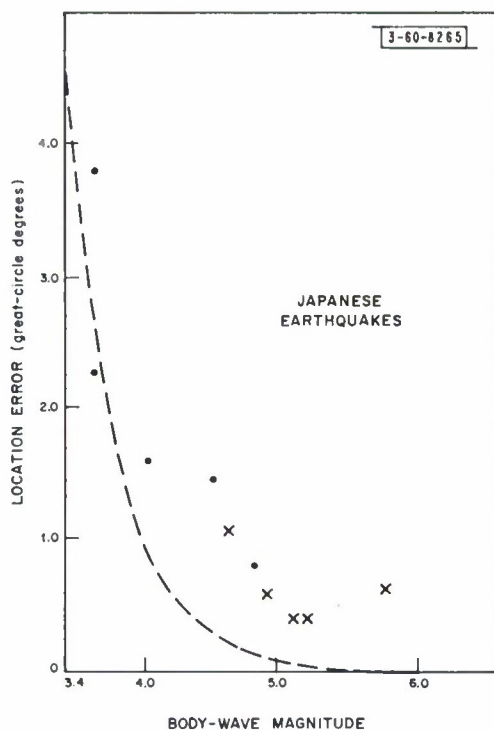


Fig. 7. Disagreement in epicenters located by beamsplitting and those obtained by local measurements (•) or from USCGS (x). Dashed curve shows theoretical minimum achievable error.

III. MONTANA ARRAY

The last six months have been spent in completing the engineering work on several changes in the Montana LASA system. Principal among these changes is the installation of eight Ling-Temco-Vought microbarographs at the centers of the A0, E1, E2, E4, F1, F2, F3, and F4 subarrays, and provisions for calibration of the LP sensors by telemetry commands from Billings. Because the delivery of components has been delayed, installation of the microbarographs will not be complete until after 31 December.

Effective 1 January 1968, the Air Force Electronic Systems Division Seismic Array Program Office will take over responsibility for operation and engineering of the Montana LASA. A series of reports describing the several recent engineering changes is in preparation. Also in preparation is a report summarizing the experiments in automated monitor/control of the Montana LASA.

R. V. Wood, Jr.
R. G. Entieknap
J. P. Densler

IV. NORWAY ARRAY

A. NORWAY SEISMIC SURVEY INSTALLATION

A number of changes were made in the seismic survey plan described in Sec. VI of the last semiannual technical summary. As of 31 December 1967, all field work for this season is complete. The following summarizes the field installations that were actually made. The map of Fig. 8 shows the three present sites.

Site 1 (Øyer):— Here the original plan called for an 18-km-diameter SP array of 20 sensors, each in a cased hole approximately 15 meters into bedrock. Substantially all drilling has been completed. Casing, cabling and installation of well-head vaults had progressed to the point where 12 sensors were connected to the recording shelter when winter weather ended field work. The Astrodata SP digital recording equipment is now operating, recording signals from the 12 available sensors. The three-component LP installation, awaiting only the arrival of its digital recording equipment, a Lincoln-built LP DART (DATA Recording Terminal), is complete at Øyer. Installation of this recording equipment and an event detector unit (designed by C. A. Wagner) which automatically generates a crude station bulletin should be completed within a month. Power and telephone cables to the Øyer recording shelter are in place, and installation of the Telex at the shelter has been promised for 15 January 1968.

Site 2 (Faldalen):— Faldalen contains a SP sensor cluster of five surface sensors (well-head vaults cemented into holes blasted into outcroppings of bedrock) plus two deep sensors in cased holes approximately 60 meters deep with hole locks on the seismometers. An LP 3-component installation has also been completed. On a low hill about one-half kilometer away, a weather station to give wind direction, wind velocity and temperature has been installed. Recordings of the SP cluster are being made on a SP DART, which can record any six of the seven available sensors. The LP 3-component data and the weather station data are being digitally recorded on an LP DART. Since the Faldalen site is experimental and of interest primarily to Lincoln Laboratory, we are recording one 11-hour SP tape per day. Running time for the LP/weather tapes is about 10 days and coverage is continuous.

Site 3 (Trysil):— The installation here consists of a 3-component LP station only. Sensors are in place and checked out, awaiting arrival of the LP DART equipment. Operational recording should start in late January 1968.

R. V. Wood, Jr.	J. R. Brown
R. G. Entieknap	J. E. Evans
J. H. Helfrich	R. M. Lerner

B. NOISE AND SIGNAL SITE SURVEY RESULTS

A plan for a noise survey was outlined in the last semiannual technical summary. The status of this plan, from a system and engineering viewpoint, has been given above. Short-period digital data from two sites, as well as analog data from Lillehammer, are now available for analysis. This work has now begun.

Several samples of SP vertical data from the LRSM station at Ringsaker have been digitized. An anti-aliasing filter at 3.0 Hz was used and data were sampled at 20 times per second. Samples

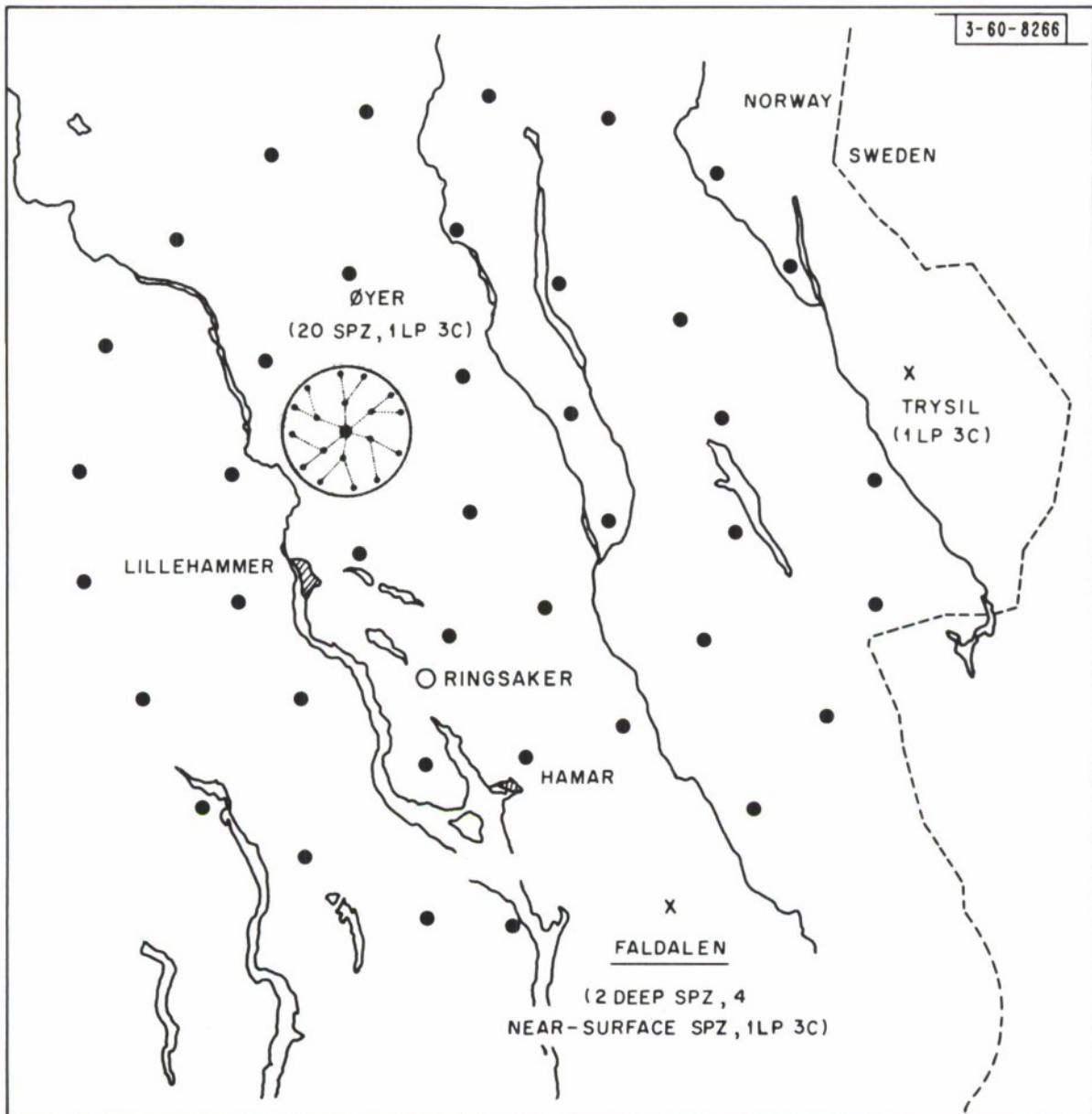


Fig. 8. Locations of the three noise survey sites in Norway: One subarray plus two simpler installations (x). Shown also are the existing LRSM station at Ringsaker (open circle) and one of a number of LP array geometries (solid dots) that have been analyzed.

of such data approximately five minutes long have been used to estimate coherency as a function of instrument separation and frequency. Frequency resolution was 0.1 Hz. Similar measurements have also been made using an analog computer at the University of Bergen. Figures 9(a-b) show plots of the digital and analog measured coherencies as a function of the product of frequency times the distance between instruments. There is a bias in the estimates which ranges from 0.0 for 1.00 coherence to about 0.2 for 0.0 coherence. Thus, estimated values of about 0.2 indicate true values of 0.0.

Higher resolution estimates of coherency have been obtained from digital data gathered at Faldalen and to a limited extent at Øyer. These data, like that obtained from digitized analog tapes, indicate that coherency is a function of distance times frequency at the Norway sites. A typical high resolution coherency at 1.8-km separation of sensors is shown in Fig. 9(c). The behavior of the coherency data at Øyer and Faldalen seem to be generally consistent with that at Ringsaker. The coherency analysis of Norway noise data is continuing.

The structure of seismic noise in Norway appears to differ somewhat from that in Montana. In Norway coherencies appear to drop off somewhat faster with distance at frequencies below 1 Hz. Spectra above 1 Hz seem less time variable in Norway than in Montana. As coherency data have accumulated, estimates of required minimum spacings between instruments in an array in Norway have fallen from 4 km (as used at Øyer) to 3 km. Direct summing of the four instruments at Faldalen (average spacing 2.6 km, minimum spacing 1.0 km) has yielded 4.5 to 5 db out of a possible 6 db for frequencies above about 0.6 Hz. This is a somewhat independent additional indication that 3-km minimum spacing should be sufficient.

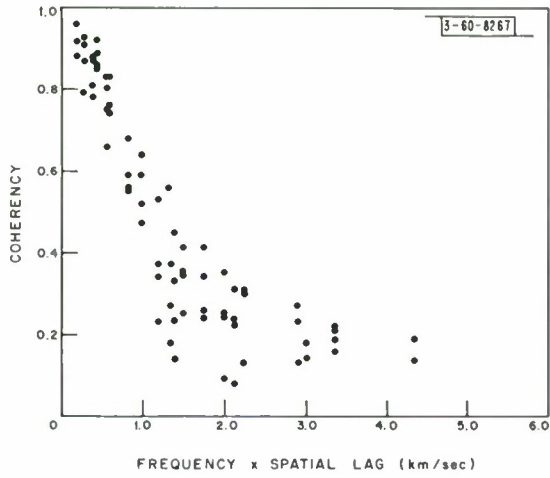
Early results from deep (60 meter) holes show no differences from spectra measured on instruments placed in surface rock outcroppings. It appears that instruments should be placed in rock but that nothing is to be gained by drilling holes up to 60 meters into the rock. This conclusion, which can have a large effect upon installation cost and difficulty, must be substantiated by further data analysis.

Frequency-wavenumber analysis has been applied to the digitized Ringsaker data. Spatially organized noise has been detected in the frequency band from 0.2 to 0.9 Hz. This noise has a time variable direction of arrival and normally appears to have a horizontal phase velocity of about 5.5 km/sec. This is too fast for surface waves and too slow for teleseismic body waves. One sample of digital data from Faldalen has also been analyzed. That also indicated the presence of noise with a similar velocity in the same frequency range.

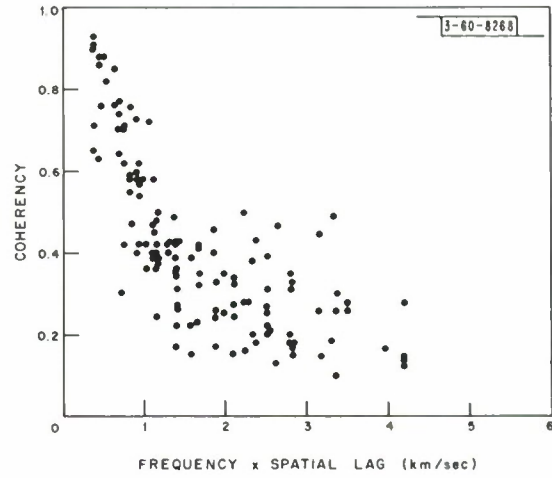
Preliminary estimates of Ringsaker station sensitivity have been obtained using the observed signal-to-noise ratios for 10 events, with locations and body-wave magnitudes reported to USCGS. This was done in two ways. Let S_T be the signal amplitude predicted by the Gutenberg Q factor working backwards from the published magnitude. Let N be the measured noise level before an event and S_m be the measured signal amplitude. The effective noise level is then $S_T N / S_m$. The effective zero-to-peak noise thus computed at 1.0 Hz ranged from 0.5 to 5.0 $\mu\mu$, with an average value of 2.2 $\mu\mu$. The value for Montana, taking the station amplitude anomaly into account is about 1 $\mu\mu$. Thus Norway appears to be a few tenths of a magnitude unit less sensitive than Montana.

This was crudely corroborated by a second procedure. Single sensor event visibility during a period of 240 hours was investigated by looking at times corresponding to all USCGS-reported

Section IV



(a) Using digitized analog tapes from Ringsaker (0.1-Hz resolution).



(b) From analog data at Ringsaker (0.1-Hz resolution).

(c) From digital data of Foldalen estimated using 1.8-km separation (0.02-Hz resolution).

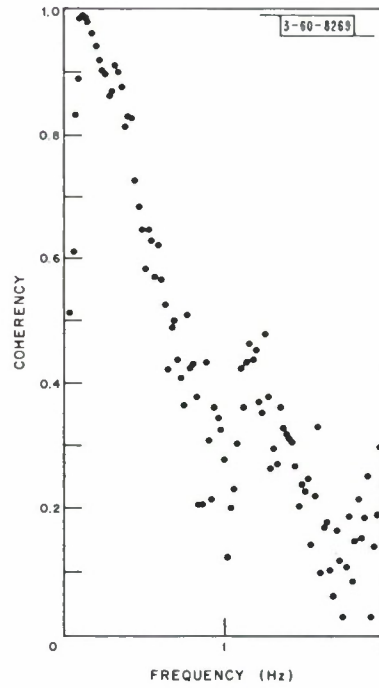


Fig. 9. Coherency estimates.

events 30° to 90° away. There were 85 such events (m_b between 3.5 and 5.9). The incremental 50-percent single-sensor detection threshold was at $4\frac{1}{2}$ USCGS magnitude.

The analysis of LP noise data will begin when all three LP noise survey sites are operational. In the meantime, the study of SP noise properties will continue.

H. Bungum (U. of Bergen)	R. T. Lacoss
J. E. Evans	R. M. Lerner
R. J. Greenfield	

C. LONG-PERIOD ARRAY DESIGN

A preliminary study of array geometry and engineering factors for an array of LP instruments in Norway has been completed and presented in a technical note.⁸ A number of alternative array geometries using between 19 and 43 elements spread somewhat uniformly on a disk were considered. (One such array is shown in Fig. 8.) The patterns corresponding to these configurations were evaluated under the assumption that delay-and-sum processing is to be used to enhance fundamental Rayleigh mode signals and reject fundamental Rayleigh wave noise. It was concluded that the distance from any element to its nearest neighbors in such an array should be in the range from 20 to 25 km. This spacing avoids spatial aliasing or pseudo-aliasing of noise propagating as surface waves or of surface waves from interfering events. Such aliasing could occur with larger spacings. Smaller spacings would reduce the velocity resolving power of the array. It was further concluded that although overall array performance is somewhat insensitive to the details of instrument placement, it is essential to check the directional characteristics of any array before installation is undertaken. Several idealized array geometries are analyzed in the report, along with some randomized arrays and some which are significant perturbations of the idealized arrays.

R. T. Lacoss
J. Capon
R. J. Greenfield

V. GEOPHYSICAL DATA HANDLING TECHNIQUES

A. DATA ANALYSIS CONSOLE

The PDP-7 computer in use at Lincoln is being improved to make "preprocessing" of seismic data more rapid and convenient. Both the hardware and the software of the PDP-7 are being upgraded. Procurement is under way for hardware improvements to be effected in about six months. These include a memory expansion from 16,000 to 32,000 words, and the addition of a faster scope display and a three-million word magnetic drum for bulk storage of tabular and archival data. The resulting structure is being called a "data analysis console," and is characterized by an emphasis on input-output convenience and man-machine interaction. The discussion which follows concerns a complete software package that has been completed for the PDP-7 as it presently exists, and which will serve as the prototype for the more powerful software of the improved PDP-7 hardware.

The console system (Fig. 10) is designed to do many of the standard data processing tasks more efficiently and accurately, and yet be quicker and easier to use than "batch processing" as found in most modern data centers. A cathode-ray tube displays the computer output quickly and in an easily interpretable manner to a human data analyst who can alter the data or give new commands to the computer via a fiber optics light pen, adjustment knobs and teletypewriter keyboard.

Useless data are not put onto paper, but are readily available for perusal if needed. Only after the data have been reduced, or after the operator decides he really wants it, is a permanent hard copy produced. This man-machine system puts a man in the feedback loop to do pattern recognition and to make decisions based on his experience as a trained seismologist or geophysicist, and to do other tasks that are very difficult for a modern electronic computer. The computer is in the loop at a place where it can outperform a human. This ability to process the results of a prior processing without punching data cards and submitting for another pass through the computing center saves a great deal of time. Some operations that take several days via the old method can be done in 15 minutes on the analysis console.

The operation and control of the console are done by a master Monitor program. This program is read in from paper tape, resides in the computer core memory thereafter, and controls the calling and execution of all the console system programs which are stored on magnetic tape. The Monitor program always knows which programs have been used and hence which physical parameters have already been determined. It saves all these data so that further processing will have access to these data. If the data have not yet been determined, the Monitor will know it and not let any further processing that depends on these data proceed. All commands to the Monitor are input to the computer simply by typing on the teletypewriter keyboard a one-character mnemonic code (given in square brackets [] in what follows). The Monitor fetches the proper program from the program tape, reads it into the core memory and executes it.

The program tape contains the console display system [D] which is the basic program from which most of the other programs are called after an initialize operation [I]. It is designed to generate a CRO display of digitized seismograms in a manner to which the seismologist is accustomed, namely up to 24 seismograms (earth motion vs time) stacked vertically, each of

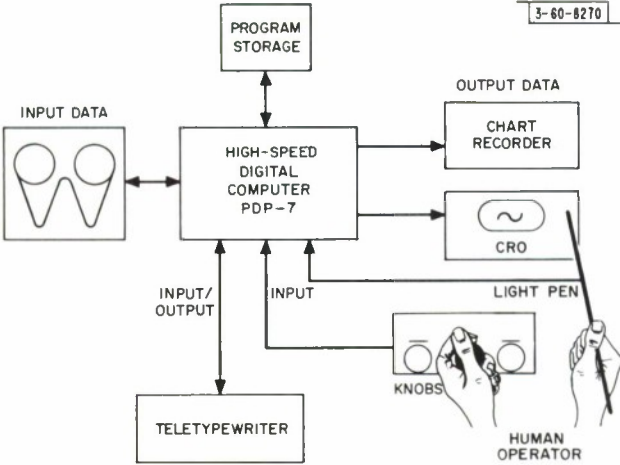


Fig. 10. Lincoln seismic data analysis console.

duration 600 samples (30 seconds of SP data or 25 to 300 seconds, at will, of LP data). Six knobs control parameters of the display, the horizontal and vertical gain of the seismograms, the vertical separation between them, their horizontal and vertical positions and a clipping level to prevent trace overlap.

The operator can use this program to visually scan his way backward and forward through the data and then pick a portion of any seismogram for further processing by other programs. This picking is done by pointing the light pen at any waveform which causes it to be saved in a "reference buffer." The contents of this reference buffer are displayed at the top of the screen with a vertical cursor appearing at the exact point in the waveform that was touched by the light pen. This "reference" trace is unaffected by any of the knobs. Thus one can, for example, move all the traces, one by one, alongside this reference by adroit manipulation of the horizontal and vertical position knobs for visual alignment and correlation. This process is used to pick arrival times for the various traces to be used for beamforming and location. By proper adjustments of the gains, this time picking can easily be done with a precision of 50 msec on SP data.

A number of programs succeed the Display program and can then be used for specific manipulations. The current ones are (more programs will be added to the system when they are written and checked out):

Location [L]:- If three or more arrival times are picked on the Display program, the best-fitting plane wave that minimizes the RMS error is calculated, and from this the horizontal phase velocity and azimuth. In addition, the relative arrival times when this plane wave would hit all 21 sites, along with the residuals to these times, are typed out. Provision is made for deleting times from any sites that may have large residuals and then repeating the calculations. (If the data are from SP seismometers, station corrections will have automatically been inserted in this calculation, and the distance from the center of LASA and the latitude and longitude of the epicenter will be computed. Also, GMT at which that portion of the seismogram corresponding to the reference cursor must have originated is calculated, assuming a focal depth of 33 km.)

Beamforming [B]:- If one or more time picks are made in the Display program, the delay-and-sum beam will be formed and placed in the reference buffer. From here, it can be filtered (see below) or used as a reference to pick arrival times from weak events. Channels that have been deleted in the Locate program just described are automatically deleted from the beam.

Constants [C]:- This program displays the reference waveform on the scope so that two points can be selected by the light pen. The GMT corresponding to each point (to the nearest 0.1 second) is then displayed on the CRT, as well as the time difference between the points and the amplitude difference in millimicrons corresponding to the two points picked (assuming normal calibration for the data displayed). The magnitude based on these last two quantities is typed out on request, if the distance has already been computed. (This assumes that the two points are peak and trough of the seismogram.) If the data are from a SP instrument, the "Q" factors are those for a depth of 33 km. If the [A] key is depressed on the teletypewriter keyboard, the cursors will be automatically moved to the nearest portion of the seismogram with zero slope. This eliminates the need for exact placement of the cursors by the light pen when determining period or peak-to-peak amplitude.

Section V

Filtering [F]:- The 21 seismograms or the reference (each 600 samples long) can be filtered. Currently, one has the choice of two filters which have been found useful in the past,⁹ a Butterworth filter [B], or a notch filter [N].

Plot [P]:- This program plots all the 21 traces on Sanborn chart recorders, providing hard copy of the interesting waveforms.

Transform [T]:- This program computes and displays 512 points on the autocorrelation function of the reference waveform, after the reference waveform has been truncated so that it is set to zero outside time interval (A, B), where A and B are set by using the light pen.

The finite Fourier transform of either the modified reference or of its autocorrelation function (both considered periodic with a period of 512 samples) can be computed and displayed (decibels vs frequency). The autocorrelation function can be truncated before this transform operation by using a knob in a manner similar to that in truncating the original waveform.

Complexity [X]:- This program computes the complexity¹⁰ of the reference trace (beam or seismogram, raw or filtered) starting at the cursor point. The complexity is defined as the integral over the first five seconds of the absolute value of the waveform (less any DC component) divided into the integral over the succeeding 30 seconds of the absolute value of the waveform.

Sonogram [S]:- This program computes and displays the sonogram (power as brightness vs frequency vertically and time horizontally¹¹) of the reference trace starting 1200 samples before the beginning of the reference buffer. The sonogram corresponds to 160 seconds of SP data, thus placing the start of the reference buffer data at the center of the sonogram display. A bank of 50 constant bandwidth filters is used, each with a $(\sin x/x)$ type frequency response, whose impulse response is a sine wave exactly 10 seconds in duration. The filters are spaced 0.1 Hz apart, over a range of 0.1 to 5.0 Hz. Each filter output is full wave rectified and passed through two low-pass filters in cascade. The first is an energy summing "integrate and dump" filter. It sums the output of the rectifier for one second, then resets itself to zero and repeats. The second filter takes these outputs sampled just before the dump (i.e., once each second) and performs "RC" type low-pass filtering. The 3-db cutoff of this filter is 0.11 Hz. The output of this bank of 50 "RC" filters is displayed in the sonogram so that one has on the scope a frequency spectrum as a function of time. The energy profile, integrated spectrum, and spectral ratio can also be calculated and displayed by this program.

P. L. Fleek R. E. Gay
L. T. Fleek L. J. Turek

B. TSUNAMI WARNING USING A SINGLE LARGE ARRAY

A study was made of the potentialities of a single large array like the Montana LASA in providing rapid tsunami warning information from earthquakes at teleseismic distance from the array. The results will be reported in a Lincoln Technical Note. It appears that speed and location accuracy of such a station are adequate. Depth determination from depth phase observation is somewhat enhanced compared to that available from a small station (as mentioned in earlier reports), but the reliability of depth determination by the combined use of depth phases, body-surface magnitude differences, and surface-wave dominant period is still

not as reliable as required. A detailed flow diagram of machine and manual array station observations for rapid tsunami warning is included in the report. In an Appendix the empirically observed limit on tsunami magnitude imposed by water depth is explained.

P. E. Green
R. J. Greenfield

VI. SEISMOLOGICAL RESEARCH

A. CRUSTAL STRUCTURE UNDER MONTANA LASA INFERRED FROM STATION ANOMALIES

The time station residuals at LASA were found to have large values, even when reduced to a reference within the array itself. The residuals were also found to have a strong dependence on the direction and distance to the epicenter. A recently published technical note¹² describes this station effect and its interpretation in some detail.

When the average values of the station residuals were plotted and contoured, they indicated that slower crustal velocities seem to be present near the center of the array while most of the outer regions of the array exhibit higher velocities. Figure 11 shows the contours of the station residuals relative to site A0. In this case the residual is defined by the equation, $R = (t_n - t_{A0}) - (t'_n - t'_{A0})$, where t_n is the measured arrival time at a subarray and t'_n is the Jeffreys-Bullen computed arrival time at that subarray.

Values of the horizontal phase velocity of teleseismic P-waves obtained by LASA were higher for events from the Aleutians-Kuriles-Japan regions than they were for events from South America. As the size of the array aperture was reduced, the difference in the phase velocities became greater, indicating that this effect was due to the crustal structure under LASA rather than to the mantle travel path of the P-wave. An example of the separation in phase velocity curves for the two major seismic regions is shown in Fig. 12. The data indicated by x are from South America while \square indicates data from the Aleutians-Japan areas.

The existence of the large station residuals and the unusual behavior of the phase velocity curves reflect the existence of a crustal anomaly of unusual character. The contours of the station residual seem to indicate that the anomaly is centered near sites D4, B4 and C1 and may have the shape of a depression in the crust-mantle boundary.

R. M. Sheppard

By applying methods similar to those of refraction seismology, it is possible to determine a non-parallel-planar structure which will give P-wave arrival time anomalies which agree with observed anomalies.

At LASA the observed anomaly, relative to the A0 subarray, at the i^{th} subarray is defined as

$$R_i^O = (t_i - t_{A0})_{\text{observed}} - (t_i - t_{A0})_{\text{Jeffreys-Bullen tables}}$$

Similarly, the anomaly predicted by the structure is

$$R_i^S = (t_i - t_{A0})_{\text{structure}} - (t_i - t_{A0})_{\text{horizontal layering only}}$$

These anomalies are dependent on the earthquake epicenter. Residuals observed at LASA indicate that the structure is, to a first approximation, delineated by non-parallel planes striking N 60 E.

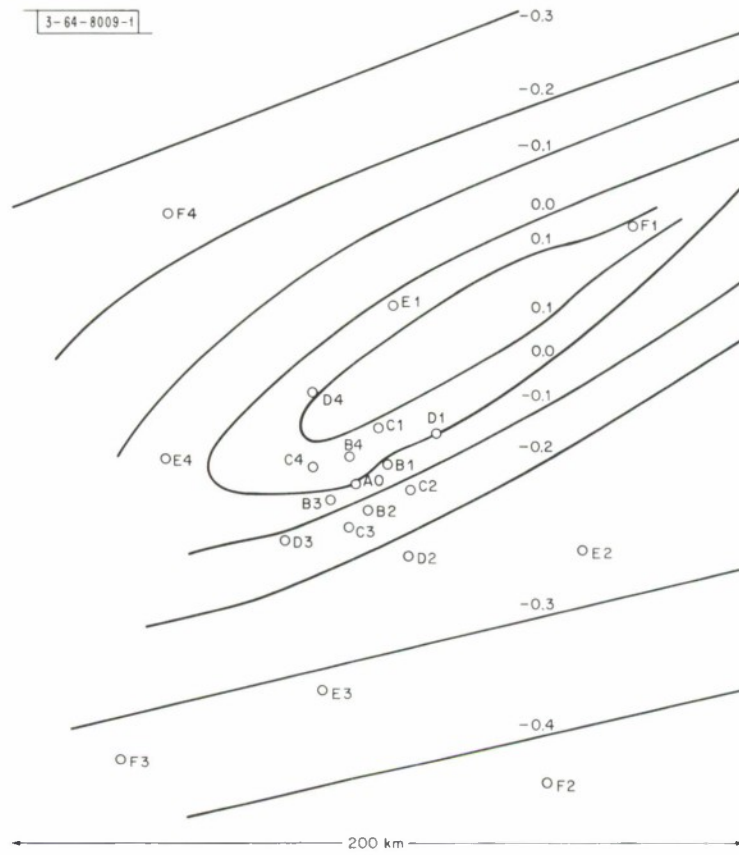


Fig. 11. Map of Montana LASA showing contours of average station residual relative to subarray A0.

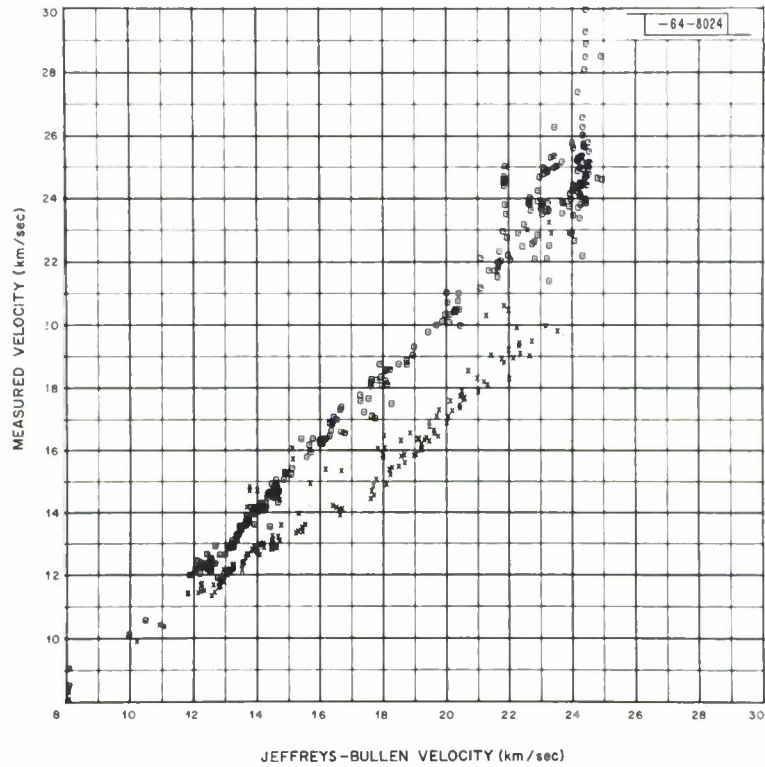


Fig. 12. Measured phase velocities vs theoretical values for Montana LASA with outside (F) subarrays deleted (x = events from southeast, □ = events from northwest).

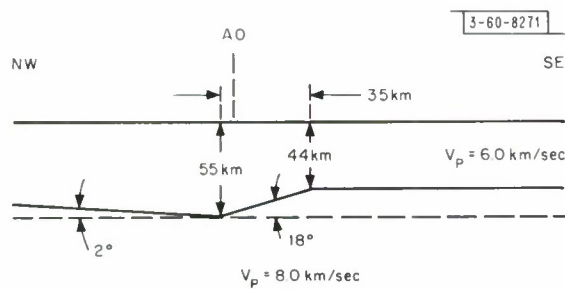


Fig. 13. Cross section of structure, composed of non-parallel-planar oriented N 60° E, which explains observed time anomalies.

Section VI

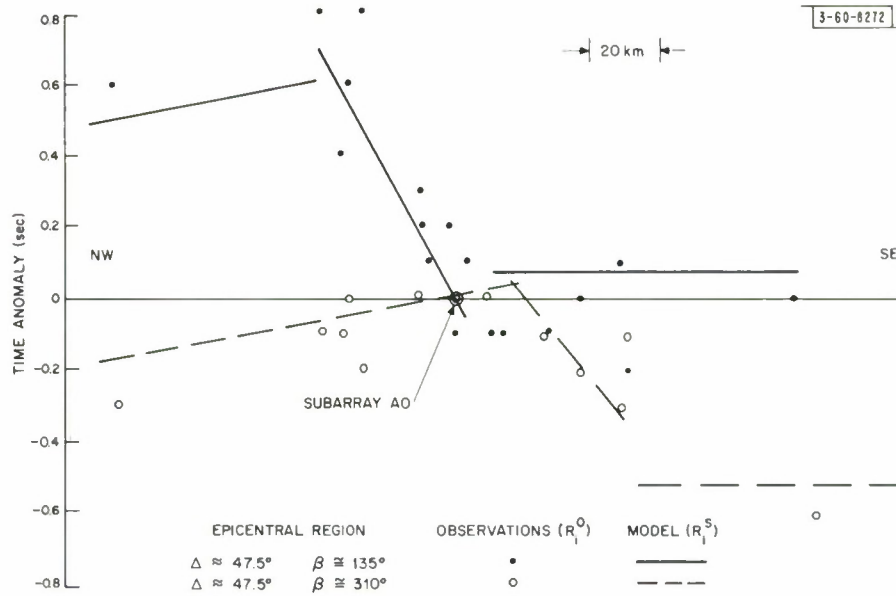
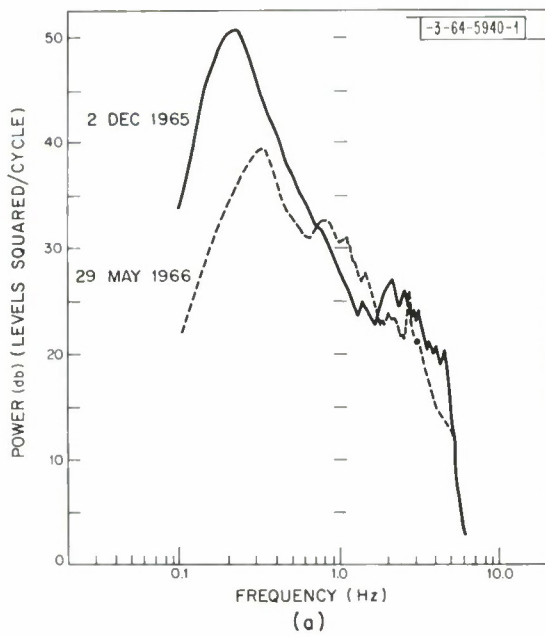
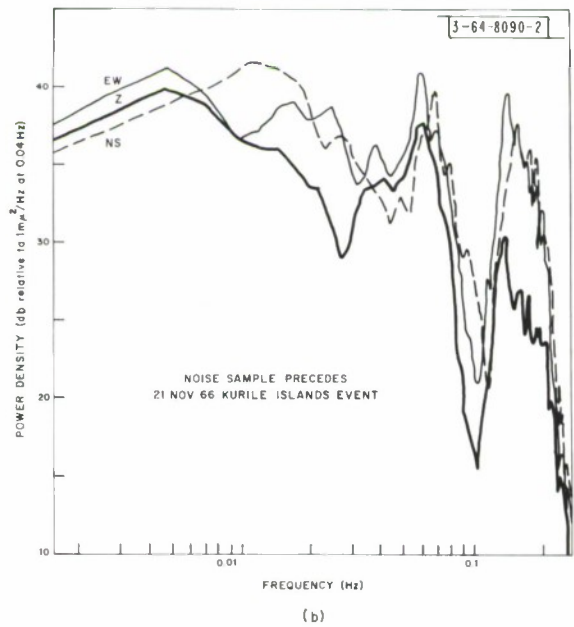


Fig. 14. P-wave arrival time anomaly relative to subarray A0 plotted vs distance S30°E. Straight lines are for the model of Fig. 13, points are observed values.



(a) Short period.



(b) Long period.

Fig. 15. Typical single-sensor noise spectra.

The cross section of such a structure giving anomalies in good agreement with the observed ones is shown in Fig. 13. Average observed anomalies for events from two epicentral regions at the LASA subarrays has been plotted vs distance perpendicular to the strike of the structure in Fig. 14. The solid and dashed lines on the figure are the anomalies predicted by the structure. The fit is observed to be quite good. The predicted anomalies are fairly sensitive to the parameters of the model; for example, using the P-velocities assumed, motion of any interface by more than 10 km results in a large disagreement with the experimental data.

R. J. Greenfield

B. MONTANA NOISE STRUCTURE

Studies of the structure of both LP and SP noise at the Montana LASA are continuing. Single-channel power spectral densities, coherencies, and power spectral densities in frequency-wavenumber space can be obtained routinely for both the LP and SP noise. The estimates of single-channel spectra and coherencies are obtained either by Fourier transforming estimated correlation functions or by using the direct segment method as described by Capon, *et al.*¹³ The spectral density at wavenumber \underline{k} and frequency f in frequency-wavenumber space is currently estimated by

$$P(\underline{k}, f) = \frac{1}{K} \sum_{m=1}^K \sum_{n=1}^K \frac{P_{mn}(f)}{\sqrt{P_{mm}(f) P_{nn}(f)}} \exp \left[i2\pi f \frac{\langle \underline{v}, \underline{r}_n - \underline{r}_m \rangle}{\langle \underline{v}, \underline{v} \rangle} \right]$$

where K is the number of seismometers, \underline{r}_n is the vector location of the n^{th} seismometer, \underline{v} is the vector phase velocity corresponding to wavenumber \underline{k} and frequency f , $\langle \dots \rangle$ denotes scalar product, and $P_{mn}(f)$ is an estimate of the cross-power spectral density between channel m and channel n . The $P_{mn}(f)$ are obtained by the direct segment method with or without weighting of the time series to obtain an improved spectral window.

Typical single-channel spectra, for SP vertical seismometers, uncompensated for instrument characteristics, are shown in Fig. 15(a). The greater power at low frequencies on 2 December 1965 is typical of late fall and winter conditions. At any given time, spectra estimated from different seismometers are similar below 1.0 Hz but are quite variable above that frequency because of local noise effects at the higher frequencies. The single-channel spectra for any one of the three LP components are much more complex than the SP spectra. The LP spectra tend to have three peaks. Figure 15(b) shows typical spectra. The relative size of the three peaks is quite variable. The size of those in the vicinity of 0.06 and 0.12 Hz tend to vary together relative to the lower frequency noise, although that at about 0.12 Hz can occasionally become large relative to that at about 0.06 Hz. The factor-of-two relationship between 0.06 and 0.12 Hz is consistent with the Longuet-Higgins theory for the generation of microseisms although, as will be noted below, the noise appears to contain Love as well as Rayleigh modes. The noise on horizontal LP instruments at LASA has often been found to be several db higher than on the verticals. This observation is based upon noise samples taken primarily from fall and winter months.

Wavenumber analysis of SP noise has yielded considerable detailed information. In general, the noise tends to be most spatially organized in two frequency bands. In the region

Section VI

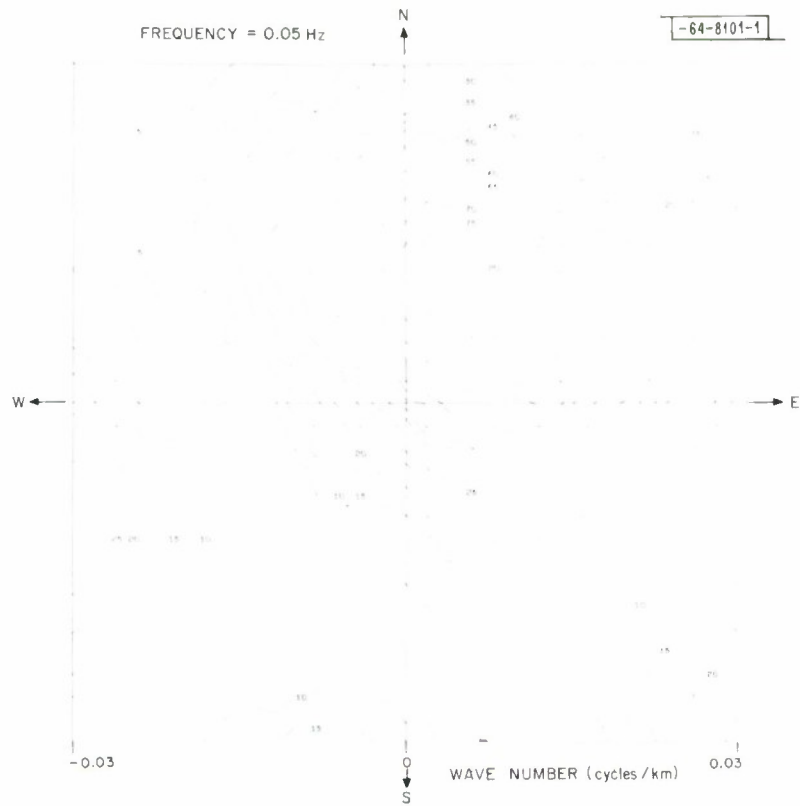


Fig. 16. Frequency-wavenumber plot of LP noise sample taken about 0500 Z 27 February 1967. Figures show percentage with respect to total noise of power on indicated contour.

from 0.2 to 0.3 Hz much of the noise propagates across the array with a horizontal phase velocity of about 3.5 km/sec. This is the approximate velocity of the first higher Rayleigh mode in the area. Although this noise occasionally comes from the west or northwest, it normally arrives from the northeast. This noise from the northeast is most likely generated by storm activity over water off the coast of Newfoundland. The occasional arrivals from the west are most likely generated by storms over the North Pacific. The SP surface waves generated by these storms are, however, severely attenuated by mountain structures between LASA and the coast. The most organized noise detected from 0.4 to 0.6 Hz normally has horizontal phase velocities corresponding to teleseismic body waves. Since only vertical instruments are used, this noise is assumed to be P-wave. In some cases the possible source region for this noise has been computed using standard travel time curves. These regions turned out to be in oceans and corresponded to low pressure areas on surface weather maps. They did not turn out to be the seismic regions of the earth as might have been expected from earlier ideas on the origin of the high velocity component. Above 0.6 Hz it has been uncommon to identify any significant amount of spatially organized noise on the SP instruments, although there is coherence for small seismometer separations.

Considerable spatial organization has been detected in all components of the LP noise by the use of frequency wavenumber analysis. An analysis has been carried out for several noise samples taken from fall and winter months in the frequency band from 0.02 to about 0.15 Hz. Significant amounts of spatially organized noise have been detected regularly at all frequencies above about 0.03 Hz. The most organized noise has tended to be at frequencies for which the single-channel power spectral density was large.

Although the degree of organization is variable, it is often large in the signal band from 0.025 to 0.05 Hz, as well as at the 0.6- and 0.12-Hz peaks. Figure 16 shows the organization of noise at 0.05 Hz as measured by nine vertical instruments in the (A) and (C) rings of LASA. The numbers in the diagram represent percentage, with respect to total noise power, of the power on the indicated contour. For example, a single plane wave propagating across the array would yield a peak value of 100 percent. Thus, the plot indicates a large amount of noise power propagating across the array from the northeast.

The phase velocities (3.7 to 3.0 km/sec) in the region from about 0.03 to about 0.15 Hz, using vertical instruments, indicate that the vertical organized noise is fundamental Rayleigh mode. The horizontal component of organized noise appears to consist of Love waves as well as the horizontal component of the Rayleigh waves. This has been verified in two ways on one noise sample for which all components of noise were highly organized. Estimates of the polarization matrix of the organized noise have been obtained. Table I shows such a matrix. Entries in the matrix are self- and cross-power spectral densities of vertical (Z), radial (R), and transverse (T) noise components. The radial and vertical components are highly correlated and 90° out of phase. The transverse component is not highly correlated with either of the other two, although it contains considerable power. The presence of significant amounts of Love energy has also been verified by performing a frequency wavenumber analysis using horizontal components pre-rotated to be transverse to the direction of noise arrival.

TABLE I POLARIZATION OF DIRECTIONAL NOISE (29 December 1966)			
	Z	R	T
Z	1025 + 0.0i	39 - 948i	-214 - 76i
R	39 + 948i	984 + 0.0i	151 - 183i
T	-214 + 76i	151 + 183i	2174 + 0.0i
$\beta = 298^\circ$ $v = 3.7 \text{ km/sec}$ $f = 0.065 \text{ Hz}$			

R. T. Lacoss
M. N. Toksöz (M.I.T.,
Geology and Geophys.
Department)

C. LASER INTERFEROMETER EARTH STRAIN MEASUREMENT

The earth undergoes a strain buildup with time ultimately leading to the rupture associated with an earthquake. The level of strain buildup required to initiate an earthquake is not known sufficiently well to be of use in anticipating the time or energy of the event, but there is evidence that shortly before an earthquake the rate of strain accumulation in a fault region may change from its previous rate (parts in 10^8 per day in active regions), a phenomenon which should be detectable with sufficiently accurate measurements. Since the strain as observed on the surface is present over a region of tens of kilometers, corresponding to the domain of the dipole stress field set up by the dislocation, the baseline of observation should be at least several kilometers long. This avoids the possibility that the instrument is measuring a local effect on a block of material of atypical properties, and also avoids other known extraneous factors such as time-variable ground water conditions.

Conventional surveying can detect these strain increments of 10^8 only if observations are made over a period of many years. By means of modulated light beams or radio phase measurements, surveyors can now achieve accuracies of parts in 10^6 in real time as the state of the art. Several groups are refining this further with the hope of achieving parts in 10^7 on open air paths.^{14, 15, 16} Variable atmospheric retardation is the problem in all these techniques. Other groups are working with evacuated tubes of kilometer lengths,¹⁷ but we feel that the expense of constructing many such installations will limit their use in the long run to a few selected paths.

In the realm of strain seismology over short baselines, measurements to several parts in 10^{10} are being made with 30-meter quartz rod strain seismographs¹⁸ and with laser interferometers,^{19, 20} the latter being restricted to short distances over which it is feasible to build enclosed tubes to avoid atmospheric effects.

We propose to face directly the problem of making measurements through the atmosphere at a degree of accuracy intermediate between the strain seismograph accuracy of 10^{-10} and the

modulated light beam figure of 10^{-6} , by the use of Michelson interferometer techniques. If this can be achieved, only fixed terminal point markers defining the many paths to be measured need be set up permanently. Our objective is to monitor the distance between points spaced 10 km to accuracies of 0.1 mm, a part in 10^8 , although a successful measurement to a part in 10^8 over 1 km would still constitute an important contribution.

The atmosphere puts three difficulties in the way of making such a measurement: (1) turbulence, (2) a slowly time-varying bulk atmospheric retardation of about 300 parts per million, and (3) a further slowly time-varying retardation of about one part per million due to water vapor. The proposed solution to these problems will now be described, followed by a discussion of current progress in attacking the first of the three.

The atmospheric turbulence causes multipath, that is, distinct ray paths that differ in path length by amounts exceeding a half wavelength of light. Such effects predominate over path lengths exceeding several hundred meters. The multipath manifests itself in large amplitude scintillations or "twinkling" and in rapid phase fluctuations exceeding 360° . A simple interferometer would not be applicable over a 10-km path because atmospheric multipath is more than one wavelength in extent. In effect, the probing accuracy is too fine grained for the medium at hand. However, a Michelson interferometer can be made to function on the envelope of the beat between two closely spaced monochromatic frequencies. Using, for instance, the lines at 6351 and 6328 Å from a He-Ne laser, a beat of 1720 GHz is obtained, corresponding to a wavelength of 0.174 mm. This "beat wavelength" represents a more suitable yardstick than does the actual wavelength of the light, since it is longer than the atmospheric multipath spread even for a path exceeding 10 km. On the other hand, it is much shorter than the modulation wavelengths currently achievable by direct modulation of the light beam,^{15, 16} about 3 cm, and is correspondingly more accurate.

The system envisaged for overcoming the multipath uses state-of-the-art components. A block diagram is given in Fig. 17. The system* has a single He-Ne laser operating simultaneously at the two wavelengths, 6351 and 6328 Å. For clarity, this is shown as two lasers in the figure. The optics are identical to those of a simple Michelson interferometer. To understand the principle of operation of the long interferometer, imagine atmospheric turbulence (which produces the multipath condition) to be absent, and consider the situation with only the 6328-Å radiation present. If one moved the distant corner reflector, a sinusoidal intensity vs position plot would result possessing a peak each half wavelength (0.00003164 cm) of displacement. Repeating the experiment with only 6351-Å radiation, intensity peaks would appear, each 0.00003176 cm. With both wavelengths present at once, the familiar beating pattern will occur as the mirror is moved. For about a hundred and forty fringes, the patterns will coincide to make the fluctuations reinforce, then the fluctuations will tend to be out of phase for a similar number of fringes, and so forth. This distance of approximately 275 fringes corresponds to 0.0087 cm, a half wavelength at the beat frequency 1720 GHz. With atmospheric turbulence present, the phases of the two sinusoids will fluctuate severely, but that of the envelope will not.

* Each of the boxes marked "synchronous detector" actually consists of a number of components described later and shown in the dotted box of Fig. 18(b).

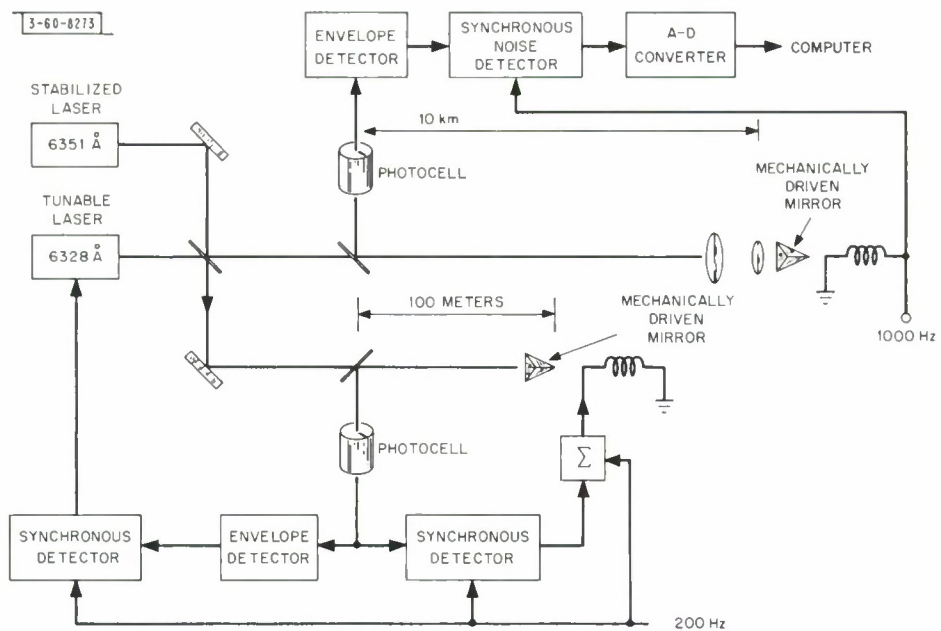


Fig. 17. Two-wavelength stabilized interferometer for earth strain measurement in presence of atmospheric multipath.

In practice, instead of moving the distant corner reflector back and forth over a short distance to bring out the beat pattern so that its phase may be measured, the two-wavelength laser (or the pair of lasers) is subjected to a small sinusoidal frequency modulation of 10^6 Hz out of the 5×10^{14} -Hz carrier frequency, thus serving three purposes simultaneously: (1) exhibiting the beat pattern, (2) chopping the light beam to avoid the need for DC amplifiers following the photo tube, (3) "tagging" the return radiation from the distant reflector so it is not confused with ambient light or light from the laser backscattered through the optics at the transmitter and/or by dust particles, etc., in the optical path.

If it were not for atmospheric retardation effects, the equipment described so far would be sufficient to measure strains to the accuracy achieved in the difference of the two laser wavelengths. However, atmospheric effects amounting to 300 parts per million and varying as much as 30 parts per million must be corrected for. Therefore, the foregoing two-wavelength interferometer is to be duplicated at another pair of optical wavelengths such as the blue-green (4900 Å) region of the argon laser or within the 11,000-Å region from still another He-Ne laser. This is to take advantage of the large dispersion of air (10 percent for 6328 to 4900 Å, 3 percent for 6328 to 11,000 Å) between these wavelengths to determine independently the total atmospheric refraction. The same optics are used for both wavelengths, with the exception of course, of the laser and the photocell. Several possibilities (e.g., prisms or dichroic mirrors) are available for "diplexing" the two lasers and photocells. This second system is not shown in the figure, since it duplicates the principle of the system already shown.

The two-color technique was first described by Prelenin.²¹ For any pair of colors selected, the relative refractivities retain a constant ratio independent of temperature or pressure. Thus, we may write the group refractive index at wavelength number one as a function of position x as

$$n_1(x) = k_1 \frac{p(x)}{\Theta(x)} + 1$$

where k_1 is a constant depending upon the precise wavelength selected, $p(x)$ is pressure as a function of x , the distance along the path, $\Theta(x)$ is temperature (absolute) as a function of x , and similarly for the second wavelength,

$$n_2(x) = k_2 \frac{p(x)}{\Theta(x)} + 1 \quad .$$

Taking c as the vacuum velocity of light, we may write the respective travel times integrated over a path length L at the two wavelengths as

$$\begin{aligned} t_1 &= \frac{1}{c} \int_0^L n_1(x) dx \\ &= \frac{k_1}{c} \int_0^L \frac{p(x)}{\Theta(x)} dx + \frac{L}{c} \end{aligned}$$

and an identical equation for t_2 except that k_1 is replaced by k_2 .

The second term in each case represents the travel time over a path length L for a vacuum, i.e.,

$$t_0 = \frac{L}{c} \quad .$$

Section VI

What is desired is to solve for the integral to find the amount by which t_1 or t_2 must be corrected to arrive at t_0 . Since the expression under the integral sign is the same in each case, we may write

$$t_2 - t_1 = \frac{k_2 - k_1}{c} \int_0^L \frac{p(x)}{\theta(x)} dx$$

and thus

$$t_0 = t_1 \frac{k_2}{k_2 - k_1} - t_2 \frac{k_1}{k_2 - k_1}$$

If, as in the example of red and blue light, k_1 and k_2 differ by about 10 percent, it is necessary to measure t_1 and t_2 (or more specifically, their difference) to at least 10 times the accuracy to which it is desired to determine t_0 . This is why a system precision of better than 10^{-9} is prescribed for achieving an overall accuracy of 10^{-8} .

The presence of water vapor introduces a further error with the two-color method which can amount to several parts per million under saturation conditions. It would be possible to use a third optical wavelength region to measure the dispersion introduced by the water vapor. However, from sensitivity considerations it appears preferable to use the 10-cm microwave region for this third wavelength. The refractivity of water vapor is 30 times as great as at optical wavelengths, making the difference in the travel times at the two wavelengths a sensitive measure of the amount of water vapor present in the propagation path. It is proposed to use a commercial surveying instrument, such as the portable Tellurometer, with little modification other than improvement of the crystal oscillator stability, for the microwave measurements. This auxiliary measurement of water vapor content over the path must correspond to an accuracy 0.3 percent in relative humidity (at 20°C) if an overall accuracy of 10^{-8} is to be achieved.

The overall measurement accuracy is specified as one part in 10^8 , and imposes a requirement on the absolute wavelength stability of the lasers to at least this value. The relative wavelengths of the different lasers in the system must be stabilized yet even more precisely. As mentioned above, the relative wavelengths of the blue and the red lasers must be stabilized to a part in 10^9 . An even more stringent requirement is imposed on the relative wavelengths of the 6351- and 6328-Å lasers. The small difference in the frequencies corresponding respectively to these two wavelengths must itself be accurate to one part in 10^9 . This imposes a requirement of 3.5 parts in 10^{12} for the stability of one of these lasers in terms of the other. Of course, the two lasers in the blue region must be similarly stabilized with respect to one another.

To summarize, the proposed system is to consist of two double-frequency lasers with associated optics, plus a microwave distance measuring equipment. This system still does not provide an unambiguous measurement of the distances since the fringe modulation envelope will be at the same position for any multiple of a half-beat wavelength, 0.087 mm. To resolve this ambiguity, it is necessary to move one of the frequencies in each of the pairs a small amount. This is most easily achieved by subjecting the laser to a magnetic field (5000 to 10,000 gauss) to induce Zeeman splitting.

At this time we have successfully demonstrated a single-wavelength Michelson interferometer at 6328 \AA over a 1.5-km path between Lincoln Building C and the L. G. Hanscom Field. The most successful earlier attempts^{22, 23} to do this resulted in observed spectral broadening of at least 18 kHz, correctly attributed to the equipment rather than the atmosphere. By careful attention to the stability of the commercial laser used in our experiment (particularly the power supply and temperature control), we have observed a frequency spread of less than 200 Hz under typical winter atmospheric conditions. These results are now in much closer agreement with theoretical values based on turbulence theory and observed amplitude fluctuation statistics.^{24, 25}

What follows is a description of the existing experimental setup, and then a presentation of the observed data. Figure 18(a) shows a Michelson interferometer schematically. Plotted below is the effect of changing the path length to one of the mirrors. The intensity as a function of displacement l follows a sinusoidal curve (displaced upward from zero by a positive bias) of one peak per wavelength.

The actual interferometer system we have used is more complicated and is shown in Fig. 18(b). The use of two beamsplitting mirrors rather than one permits greater flexibility in selecting beam sizes and intensities. The short-path beam is made about 10,000 times as intense as the long-path beam in order to increase detection efficiency, a procedure at variance with the usual interferometer practice of making the two beams of approximately equal strengths to maximize the ratio of the intensities of the fringe peaks and troughs. The end reflectors are corner cube reflectors, avoiding the need for their accurate orientation. The beamsplitter mirrors still must be oriented to a fractional wavelength accuracy over the useful beam diameter (several millimeters).

The signal processing block diagram, also included in Fig. 18(b), is based on the need to obtain unambiguous phase information* in the presence of variations of the intensity of the returned laser beam and of the ambient background illumination. The electrical outputs are compatible with the real-time inputs to our PDP-7 computer.

The optical path length of the interferometer is "dithered" or swept over several wavelengths at 1000 times per second.†

That is,

$$l(t) = l_0 + M \cos pt$$

where

l = path length (optical)

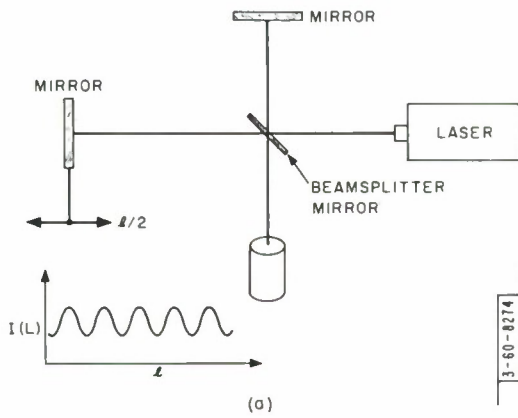
l_0 = path length at center position of mirror

M = amplitude of dither

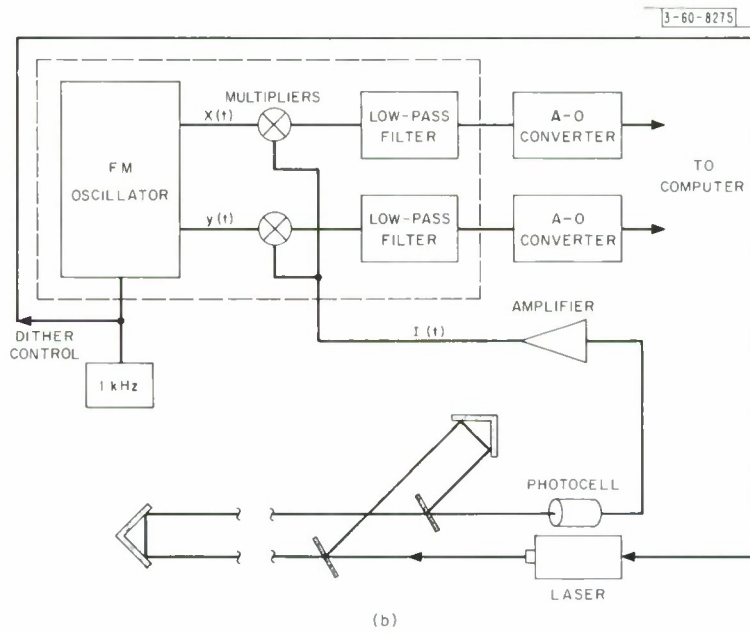
* The phase ambiguity modulo 360° of course cannot be eliminated without using two or more laser wavelengths simultaneously or in rapid alternation.

† This can be accomplished either by moving the remote mirror sinusoidally back and forth or by shifting the frequency of the laser by a small amount (about 10^6 Hz out of a carrier frequency of 5×10^{14} Hz). Although we have used the latter procedure, the discussion to follow will proceed as though the actual mirror were moved. Figures 17 and 18(a) show the mirror actually being moved. Figure 18(b) shows the experimental setup as it actually exists.

Section VI



(a) Elementary Michelson interferometer.



(b) Actual interferometer.

Fig. 18. Block diagrams explaining loser strain experiments to date.

p = dither rate, $2\pi \times 10^3$ radian/second in this case

t = time.

The intensity I as a function of path length is

$$I(\ell) = \frac{2\pi}{\lambda} \ell + \text{const}$$

and as a function of time, the intensity $I(t)$ is (disregarding the constant)

$$I(t) = \cos\left[\frac{2\pi}{\lambda} (\ell_0 + M \cos pt)\right]$$

We may normalize to put the equation in a more familiar form by setting $(2\pi/\lambda) \ell_0 = \phi$, the phase angle for a path length ℓ_0 , and $(2\pi/\lambda) M = m$, the phase modulation index introduced by the dithering of the path length, giving

$$I(t) = \cos(m \cos pt + \phi)$$

This represents the expression for an FM signal at zero center frequency and modulation index m . What we are interested in is recovering the phase ϕ . This could be accomplished by cross correlating the intensity $I(t)$ against a locally generated waveform of the same type as above and observing the value of ϕ that yields a maximum correlation. The same result can be accomplished by taking the cross correlation for just two values of ϕ : 0 and $-\pi/2$. That is, we can use two functions

$$X(t) = \cos(m \cos pt)$$

$$Y(t) = \sin(m \cos pt)$$

where $X(t)$ and $Y(t)$ are quasi-orthogonal, approaching true orthogonality for large m . (The orthogonal interval is one period $2\pi/p$.)

Under these circumstances, if we define the cross-correlation terms,

$$x = \langle X(\ell) I(t) \rangle_{av}$$

$$y = \langle Y(t) I(t) \rangle_{av}$$

the phase angle is

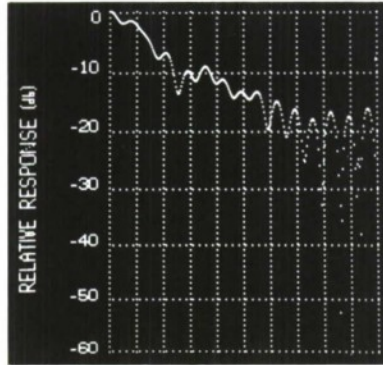
$$\phi = \text{arc tan } \frac{y}{x},$$

where the correct quadrant assignment of ϕ is based on the signs of the individual quantities x and y .

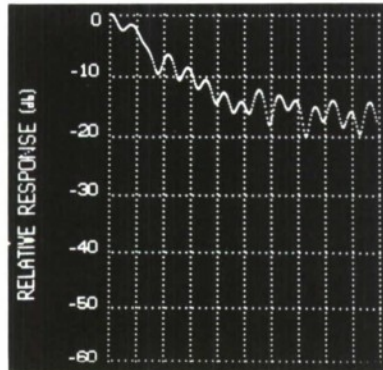
It should be noted that the above analysis assumes that ℓ_0 or ϕ is essentially unchanged over the time interval $2\pi/p$, corresponding to one cycle of the dither frequency. It is necessary to make this frequency sufficiently high (i.e., the time interval $2\pi/p$ sufficiently short) to ensure this. This choice of 1000 Hz appears to fulfill this requirement. This is also conveniently taken as the sampling rate for the digitized forms of x and y fed into the computer.

The most important parameter to be measured from a single-frequency interferometer measurement is the RMS rate of fringe crossing. This is equivalent in a coherent laser communication problem to the RMS frequency spread introduced by the atmosphere (and by any

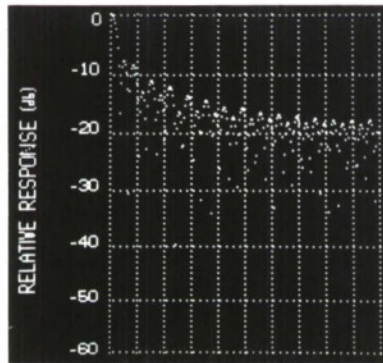
-60-8276(a-c)



(a)



(b)



(c)

Fig. 19. Spectra of atmospheric fluctuations at 6328 Å. (a) Total received signal, (b) phase only, (c) amplitude only. Vertical lines are 50 Hz apart.

frequency instability in the laser) in an equivalent one-way path. The frequency spreading can result either from amplitude- or phase-modulation of the signal, or, more generally, a combination of both.

Figure 19(a) is a computer plot of the spectrum of the received fringes for a run of 19 December 1967. Figure 19(b) shows the spectrum of the phase fluctuations only, i.e., the same data hard limited. Figure 19(c) is a plot of the spectrum of the amplitude fluctuations, i.e., the original signal envelope detected. In interpreting these plots, it is necessary to correct for an equipment roll-off of 6 db/octave due to low-pass filtering above 50 Hz and a system noise level at -20 db from the peak. The observed RMS spectral spread of the total signal is about 200 Hz, of the phase fluctuations about 200 Hz, and of the amplitude fluctuations 100 Hz.

These observed spectral widths are consistent with the system requirements for interferometric strain measurements to a part in 10^9 . However, they appear somewhat greater (by a factor of three) than predicted, based on the theoretical results of Refs. 24 and 25. It is very likely that short-term laser instabilities are contributing at least a part of this spread. There are methods for checking directly such short-term laser instabilities, and the stabilities could be improved drastically if necessary by a quieter environment than that available in the Lincoln Building C environment.

The design and procurement of elements for adding the 6351-Å wavelength are now under way.

E. Gehrels

VII. CUMULATIVE LIST OF PUBLICATIONS

Reports

- N. M. Abramson, "Further Considerations in the Use of Large Seismometer Arrays," Group Report 64G-6, Lincoln Laboratory, M.I.T. (14 November 1963), DDC 424594, H-550.
- M. Adler, "Noise and Low-Frequency Amplifiers," Technical Note 1965-52, Lincoln Laboratory, M.I.T. (21 December 1965), DDC 476983, H-695.
- H. W. Briscoe, J. Capon, P. L. Fleck, Jr., P. E. Green, Jr., R. J. Greenfield and E. J. Kelly, Jr., "Interim Report on Capabilities of the Experimental Large Aperture Seismic Array," Technical Note 1966-16, Lincoln Laboratory, M.I.T. (24 February 1966), DDC 631285, H-714.
- H. W. Briscoe and R. M. Sheppard, "A Study of the Capability of a LASA to Aid the Identification of a Seismic Source," Technical Note 1966-38, Lincoln Laboratory, M.I.T. (11 July 1966), DDC 637166, H-731.
- J. Capon and R. J. Greenfield, "Asymptotically Optimum Multidimensional Filtering for Sampled-Data Processing of Seismic Arrays," Technical Note 1965-57, Lincoln Laboratory, M.I.T. (17 December 1965), DDC 626180, H-690.
- J. Capon, R. J. Greenfield and R. J. Kolker, "A Frequency-Domain Synthesis Procedure for Multidimensional Maximum-Likelihood Processing of Seismic Arrays," Technical Note 1966-29, Lincoln Laboratory, M.I.T. (6 May 1966), DDC 634233, H-724.
- J. Capon, R. J. Greenfield and R. T. Lacoss, "Off-Line Signal Processing Results for the Large Aperture Seismic Array," Technical Note 1966-37, Lincoln Laboratory, M.I.T. (11 July 1966), DDC 637016, H-730.
- _____, "Design of Seismic Arrays for Efficient On-Line Beamforming," Technical Note 1967-26, Lincoln Laboratory, M.I.T. (27 June 1967), DDC 655142, H-850.
- _____, "Long-Period Signal Processing Results for Large Aperture Seismic Array," Technical Note 1967-50, Lincoln Laboratory, M.I.T. (15 November 1967), H-869.
- J. F. Claerbout, "A Summary, by Illustrations, of Least Squares Filters with Constraints," Technical Note 1966-7, Lincoln Laboratory, M.I.T. (31 January 1966), DDC 629968, H-708.
- P. L. Fleck, Jr., "FASTABUL (A Fast Automatic STation BULLETIN Program)," Technical Note 1967-3, Lincoln Laboratory, M.I.T. (6 January 1967), DDC 646207, H-760.
- E. Gehrels, "A Review of Long-Range Earth Strain Measurement Techniques for Providing Earthquake Warning," Technical Note 1965-62, Lincoln Laboratory, M.I.T. (13 December 1965), DDC 625817, H-689.
- E. Gehrels and L. G. Kraft, "A Computer Signal-Processing Approach for the Shapiro Fourth Test of the General Theory of Relativity," Technical Note 1966-23, Lincoln Laboratory, M.I.T. (2 September 1966), DDC 639733, H-741.
- P. E. Green, Jr., "A Large Aperture Seismic Array," Group Report 1965-1, Lincoln Laboratory, M.I.T. (6 January 1965), DDC 609851, H-628.
- P. E. Green, Jr. and R. V. Wood, Jr., "Large Aperture Seismic Array Capabilities," Technical Report 421, Lincoln Laboratory, M.I.T. (12 July 1966), DDC 639197.
- E. J. Kelly, Jr., "The Representation of Seismic Waves in Frequency-Wave Number Space," Group Report 1964-15, Lincoln Laboratory, M.I.T. (6 March 1964), DDC 433611, H-569.

Section VII

- E. J. Kelly, Jr., "Limited Network Processing of Seismic Signals," Group Report 1964-44, Lincoln Laboratory, M.I.T. (4 September 1964), DDC 447220, H-604.
- _____, "A Comparison of Seismic Array Processing Schemes," Technical Note 1965-21, Lincoln Laboratory, M.I.T. (14 June 1965), DDC 618017, H-656.
- _____, "LASA On-Line Detection, Location and Signal-to-Noise Enhancement," Technical Note 1966-36, Lincoln Laboratory, M.I.T. (1 July 1966), DDC 636144, H-727.
- _____, "Response of Seismic Arrays to Wide-Band Signals," Technical Note 1967-30, Lincoln Laboratory, M.I.T. (29 June 1967), DDC 656344, H-852.
- E. J. Kelly, Jr., and M. J. Levin, "Signal Parameter Estimation for Seismometer Arrays," Technical Report 339, Lincoln Laboratory, M.I.T. (8 January 1964), DDC 435489, H-643.
- R. T. Lacoss, "Geometry and Patterns of Large Aperture Seismic Arrays," Technical Note 1965-64, Lincoln Laboratory, M.I.T. (31 December 1965), DDC 628148, H-701.
- R. T. Lacoss, J. Capon and R. J. Greenfield, "Preliminary Design of a Long-Period Seismic Array for Norway," Technical Note 1968-4, Lincoln Laboratory, M.I.T. (January 1968).
- M. J. Levin, "Bounds on the Inverse of a Positive Definite Symmetric Matrix," Group Report 1964-67, Lincoln Laboratory, M.I.T. (20 November 1964), DDC 452772, H-622.
- _____, "A Method for Power Spectrum Parameter Estimation," Group Report 1965-8, Lincoln Laboratory, M.I.T. (10 February 1965), DDC 612796, H-633.
- R. Price, "Statistical Synthesis of a pP-Wave Enhancer," Technical Note 1965-22, Lincoln Laboratory, M.I.T. (14 June 1965), DDC 617951, H-655.
- _____, "An Approach to Estimation in Seismic Equalization," Technical Note 1965-24, Lincoln Laboratory, M.I.T. (28 June 1965), DDC 619020, H-663.
- J. S. Richters, "The Application of Analysis of Variance to the Seismic Discrimination Problem," Group Report 1964-60, Lincoln Laboratory, M.I.T. (3 November 1964), DDC 451871, H-618.
- R. M. Sheppard, Jr., "Values of LASA Time Station Residuals, Velocity and Azimuth Errors," Technical Note 1967-44, Lincoln Laboratory, M.I.T. (8 September 1967), DDC 662004, H-866.
- R. M. Sheppard, Jr., E. J. Kelly, Jr. and H. W. Briscoe, "Some Observations of Weak Japanese Earthquakes at the Montana LASA," Technical Note 1968-3, Lincoln Laboratory, M.I.T. (12 January 1968).

Journal Articles

- H. W. Briscoe and P. L. Fleck, Jr., "Data Recording and Processing for the Experimental Large Aperture Seismic Array," Proc. IEEE, 53, 1852 (December 1965), DDC 632147.
- _____, "A Real-Time Computing System for LASA," Proc. Spring Joint Computer Conference (1966), DDC 642202.
- J. Capon, R. J. Greenfield and R. J. Kolker, "Multidimensional Maximum-Likelihood Processing of a Large Aperture Seismic Array," Proc. IEEE, 55, 192 (February 1967), DDC 651722.
- J. Capon, R. J. Greenfield, R. J. Kolker and R. T. Lacoss, "Short-Period Signal Processing Results for the Large Aperture Seismic Array," Geophysics (scheduled for Vol. 33, No. 3 June 1968).
- R. A. Frosch and P. E. Green, Jr., "The Concept of a Large Aperture Seismic Array," Proc. Roy. Soc. A 290, No. 1422 (March 1966).

P. E. Green, Jr., R. A. Frosch and C. F. Romney, "Principles of an Experimental Large Aperture Seismic Array (LASA)," Proc. IEEE, 53, 1821 (December 1965), DDC 632150.

P. E. Green, Jr., E. J. Kelly, Jr. and M. J. Levin, "A Comparison of Seismic Array Processing Methods," Second I.U.G.G. Meeting, Rehovot, Israel, 13 - 23 June 1965, Geophys. J. R. Astr. Soc., 11, 67 (1966), DDC 649184.

P. E. Green, Jr., "Seismic Data Collection," Proc. IBM Scientific Computing Symposium on Environmental Sciences, November 14 - 16, Thomas J. Watson Research Center, Yorktown Heights, N. Y. (1966), DDC 661155.

R. T. Lacoss, "Adaptive Combining of Wide-Band Array Data for Optimal Reception," accepted by IEEE Trans. on Geophys. Electronics.

M. J. Levin, "Least-Squares Array Processing for Signals of Unknown Form," Radio Electron. Eng. 29, 213 (April 1965), DDC 618772.

R. V. Wood, Jr., R. G. Enticknap, C. S. Lin and R. M. Martinson, "Large Aperture Seismic Array Signal Handling System," Proc. IEEE, 53, 1844 (December 1965), DDC 632146.

REFERENCES

1. J. Capon, R.J. Greenfield and R.T. Lacoss, "Long-Period Signal Processing Results for the Large Aperture Seismic Array," Technical Note 1967-50, Lincoln Laboratory, M.I.T. (15 November 1967).
2. R.C. Lieberman, C.Y. King, J.N. Brune and P.W. Pomeroy, "Excitation of Surface Waves by the Underground Nuclear Explosion of Longshot," *J. Geophys. Res.* 71, 4333 (September 1966).
3. P.D. Marshall, E.W. Carpenter, A. Douglas and J.B. Young, "Some Seismic Results of the Longshot Explosion," Report 0-67/66, Atomic Weapons Research Establishment, United Kingdom Atomic Energy Authority (1966).
4. R.C. Lieberman and P.W. Pomeroy, "Excitation of Surface Waves by Events in Southern Algeria," *Science*, 156 (26 May 1967).
5. P.E. Green, Jr. and R.J. Greenfield, report in preparation.
6. P.D. Marshall, United Kingdom Atomic Weapons Research Establishment, private communication, 1967.
7. Semiannual Technical Summary Report to the Advanced Research Projects Agency on Seismic Discrimination, Lincoln Laboratory, M.I.T. (30 June 1967), DDC 657327; see Sec. III-D.
8. R.T. Lacoss, J. Capon and R.J. Greenfield, "Preliminary Design of a Long-Period Seismic Array for Norway," Technical Note 1968-4, Lincoln Laboratory, M.I.T., in preparation.
9. J. Capon, R.J. Greenfield and R.T. Lacoss, "Off-Line Signal Processing Results for the Large Aperture Seismic Array," Technical Note 1966-37, Lincoln Laboratory, M.I.T. (11 July 1966), DDC 637016, H-730; see Figs. I(a) and (b).
10. Semiannual Technical Summary Report to the Advanced Research Projects Agency on Seismic Discrimination, Lincoln Laboratory, M.I.T. (31 December 1966), DDC 646677; see Sec. II-C.
11. *Op. cit.* (30 June 1964), DDC 443444; see Sec. III.
12. R.M. Sheppard, Jr., "Values of LASA Time Station Residuals, Velocity and Azimuth Errors," Technical Note 1967-44, Lincoln Laboratory, M.I.T. (8 September 1967), DDC 662004, H-866.
13. J. Capon, R.J. Greenfield and R.J. Kolker, "Multidimensional Maximum-Likelihood Processing of a Large Aperture Seismic Array," *Proc. IEEE*, 55, No. 2, 192 (February 1967).
14. P.L. Bander, "Laser Measurements of Long Distances," *Proc. IEEE*, 55, No. 6, 1039 (June 1967).
15. J.C. Owens, "Recent Progress in Optical Distance Measurement: Lasers and Atmospheric Dispersion," *Proceedings I. A. G. Symposium on Figure of the Earth and Refraction*, Vienna, March 1967.
16. M.C. Thompson and H.B. Jones, "Correction of Atmospheric Errors in Electronic Measurements of Earth Crust Movements," *Bull. Seism. Soc. Am.*, 57, No. 4, 641 (August 1967).
17. V. Vali, Boeing Scientific Research Laboratories, private communication.
18. H. Benioff, "Fused-Quartz Extensometer for Secular, Tidal and Seismic Strains," *Bull. Geolog. Soc. Am.*, 70, 1019 (1959).
19. V. Vali, R.S. Kraystad, and R.W. Moss, "Laser Interferometer for Earth Strain Measurements," *Rev. Sci. Instr.* 36, No. 9, 1352 (1965).
20. H.J. Van Veen, J. Sarino and L.E. Alsop, "An Optical Maser Strain Meter," *J. Geophys. Res.* 71, 5478 (15 November 1966).

21. M. T. Prelenin, "Light Modulating Method for Determining Average Index of Refraction of Air Along a Line," Tr. Tsentr. Nauchno-Issled. Inst. Geodezii Aerozemki i Kartagrofii, D.A. Slobodchikov, Ed. Moscow: Izdatel'stvo Geodezicheskoy Literaturi, 1957, pp. 127 – 130.
22. W. E. Ahearn and J. W. Crowe, "Linewidth Measurement of C.W. Gallium Arsenide Lasers at 77°K," IEEE J. Quant. Electron. QE-2, No. 9 (September 1966).
23. I. Goldstein, P. R. Miles and A. Chabot, "Heterodyne Measurements of Light Propagation Through Atmospheric Turbulence," Proc. IEEE, 53, 1172 (September 1965).
24. V. I. Tatarski, Wave Propagation in a Turbulent Medium (McGraw-Hill, New York, 1961).
25. D. L. Fried, "Atmospheric Modulation Noise in an Optical Heterodyne Receiver," IEEE J. Quant. Electron. QE-3, No. 6, 213 (June 1967).

